

Recent results in lattice EFT for nuclei

Dean Lee (NC State)

Nuclear Lattice EFT Collaboration

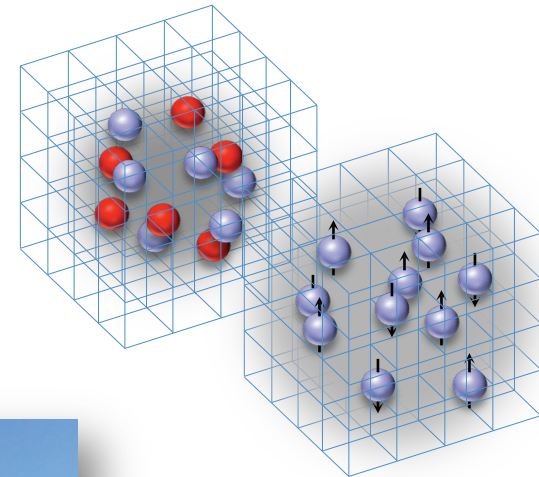
Centro de Ciencias de Benasque Pedro Pascua

Bound states and resonances in EFT

and Lattice QCD calculations

Benasque, Spain

July 23, 2014



Outline

Overview of lattice effective field theory

Light quark mass dependence of helium burning

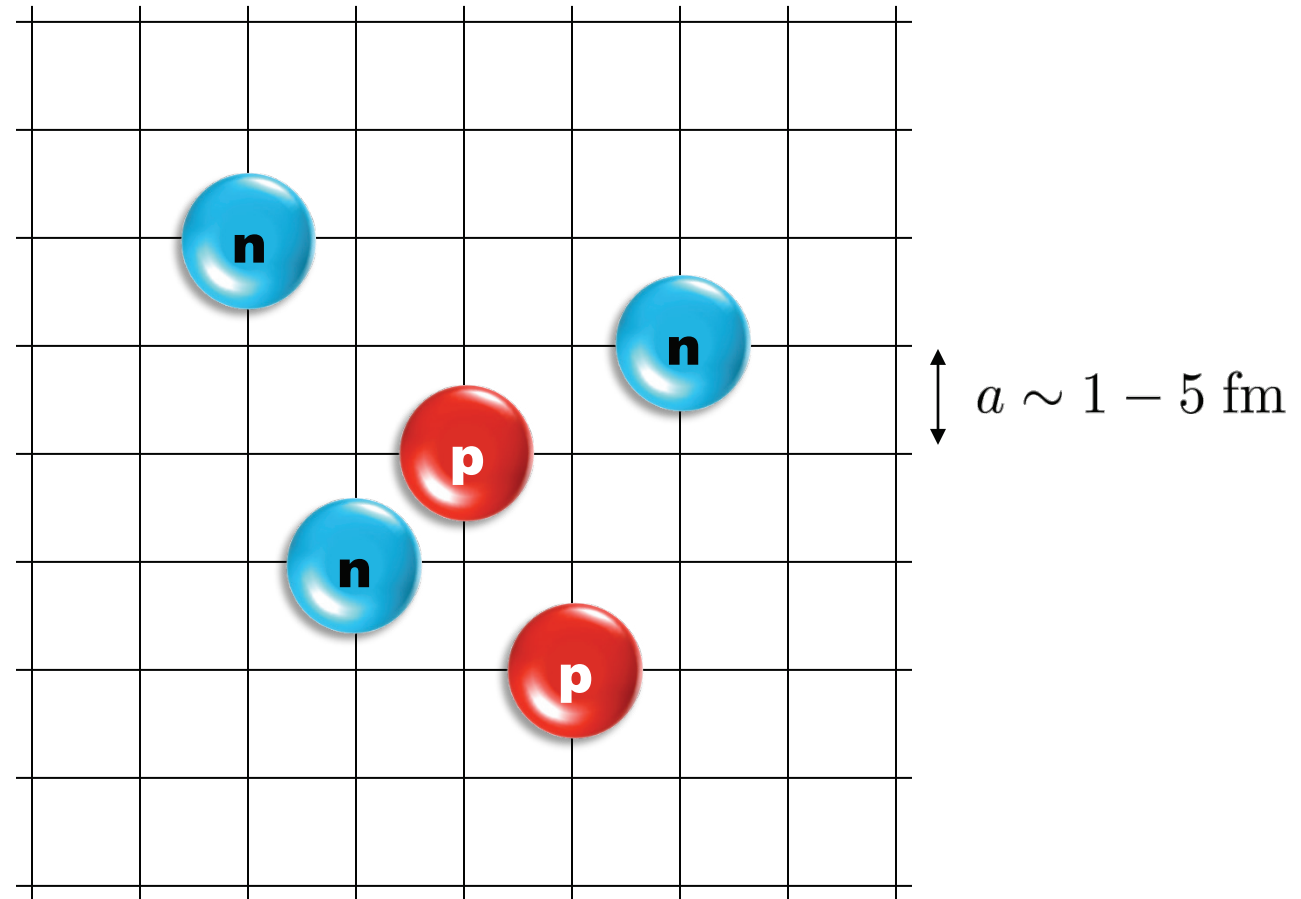
Oxygen-16 structure and spectrum

First simulations of neutron-rich matter

Adiabatic projection method

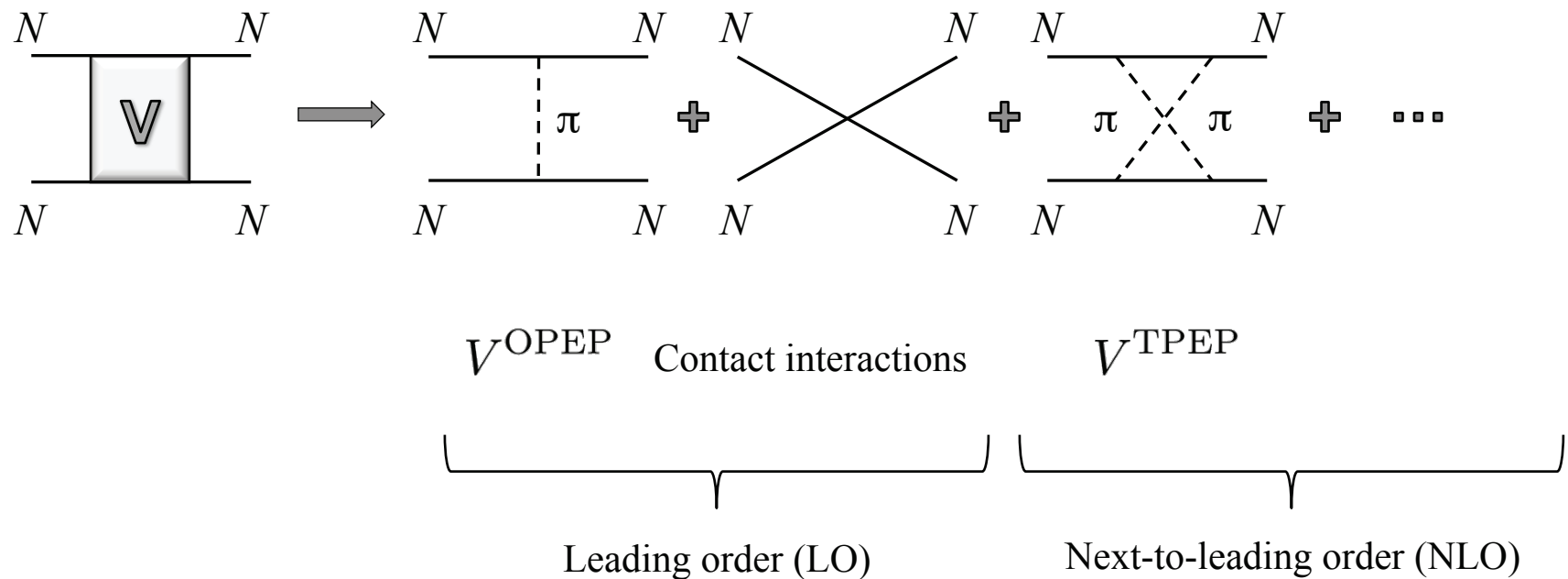
Summary and future directions

Lattice effective field theory



Low energy nucleons: Chiral effective field theory

Construct the effective potential order by order



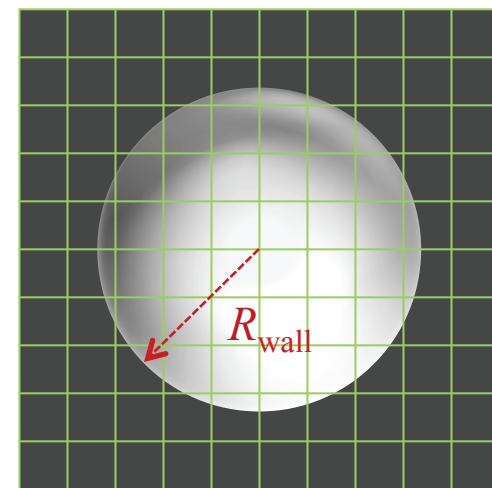
Physical
scattering data

Unknown operator
coefficients

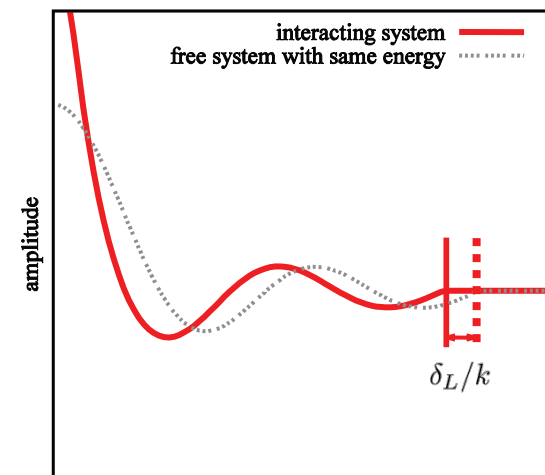
Spherical wall method

Borasoy, Epelbaum, Krebs, D.L., Meißner,
EPJA 34 (2007) 185

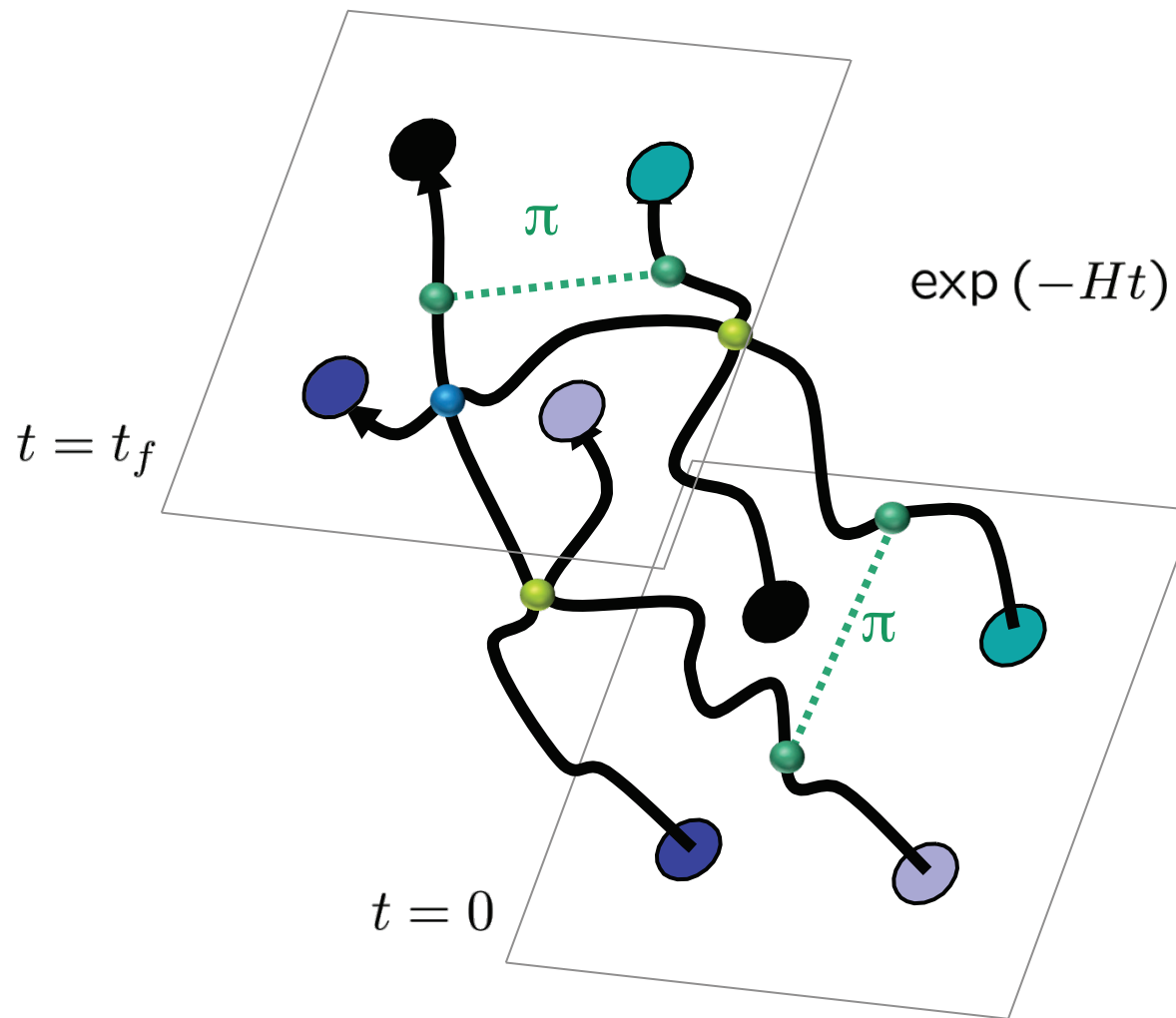
Spherical wall imposed in the center of mass
frame



Representation	J_z	Example
A_1	$0 \bmod 4$	$Y_{0,0}$
T_1	$0, 1, 3 \bmod 4$	$\{Y_{1,0}, Y_{1,1}, Y_{1,-1}\}$
E	$0, 2 \bmod 4$	$\left\{Y_{2,0}, \frac{Y_{2,-2}+Y_{2,2}}{\sqrt{2}}\right\}$
T_2	$1, 2, 3 \bmod 4$	$\left\{Y_{2,1}, \frac{Y_{2,-2}-Y_{2,2}}{\sqrt{2}}, Y_{2,-1}\right\}$
A_2	$2 \bmod 4$	$\frac{Y_{3,2}-Y_{3,-2}}{\sqrt{2}}$



Euclidean time projection

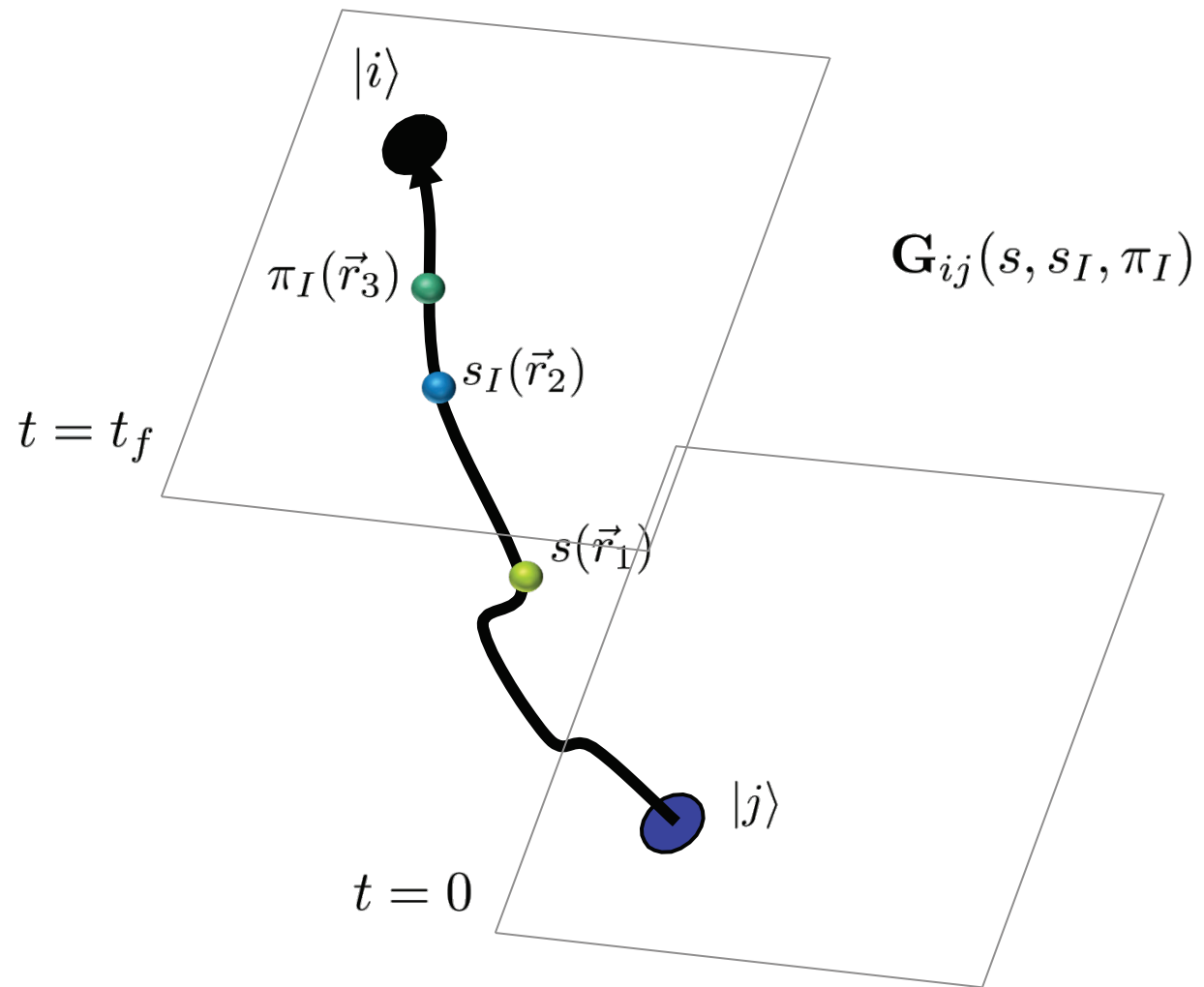


Auxiliary field method

We can write exponentials of the interaction using a Gaussian integral identity

$$\exp \left[-\frac{C}{2} (N^\dagger N)^2 \right] \quad \times (N^\dagger N)^2 \\ = \sqrt{\frac{1}{2\pi}} \int_{-\infty}^{\infty} ds \exp \left[-\frac{1}{2}s^2 + \sqrt{-C} s(N^\dagger N) \right] \quad \rangle s N^\dagger N$$

We remove the interaction between nucleons and replace it with the interactions of each nucleon with a background field.



Schematic of lattice Monte Carlo calculation

$$\boxed{} = M_{\text{LO}} \quad \boxed{} = M_{\text{approx}} \quad \boxed{} = O_{\text{observable}}$$

$$\boxed{} = M_{\text{NLO}} \quad \boxed{} = M_{\text{NNLO}}$$

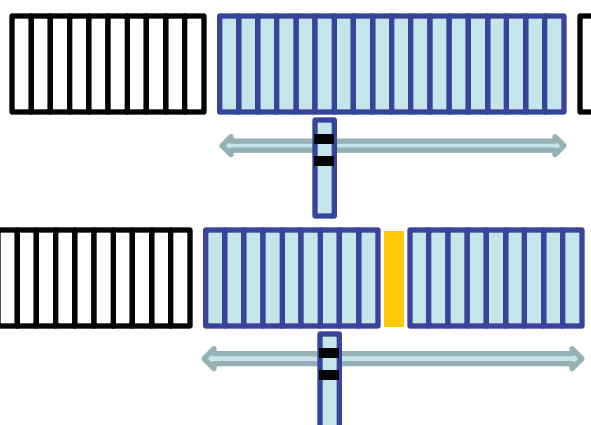
Hybrid Monte Carlo sampling

$$\rightarrow Z_{n_t, \text{LO}} = \langle \psi_{\text{init}} | \boxed{} \boxed{} \boxed{} | \psi_{\text{init}} \rangle$$

$$Z_{n_t, \text{LO}}^{\langle O \rangle} = \langle \psi_{\text{init}} | \boxed{} \boxed{} \boxed{} \boxed{} | \psi_{\text{init}} \rangle$$

$$e^{-E_{0, \text{LO}} a_t} = \lim_{n_t \rightarrow \infty} Z_{n_t+1, \text{LO}} / Z_{n_t, \text{LO}}$$

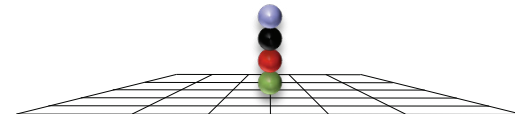
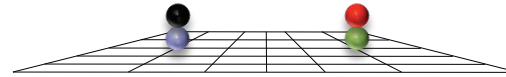
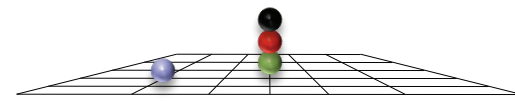
$$\langle O \rangle_{0, \text{LO}} = \lim_{n_t \rightarrow \infty} Z_{n_t, \text{LO}}^{\langle O \rangle} / Z_{n_t, \text{LO}}$$

$$Z_{n_t, \text{NLO}} = \langle \psi_{\text{init}} | \begin{array}{|c|c|c|} \hline \text{black} & \text{blue} & \text{black} \\ \hline \end{array} | \psi_{\text{init}} \rangle$$


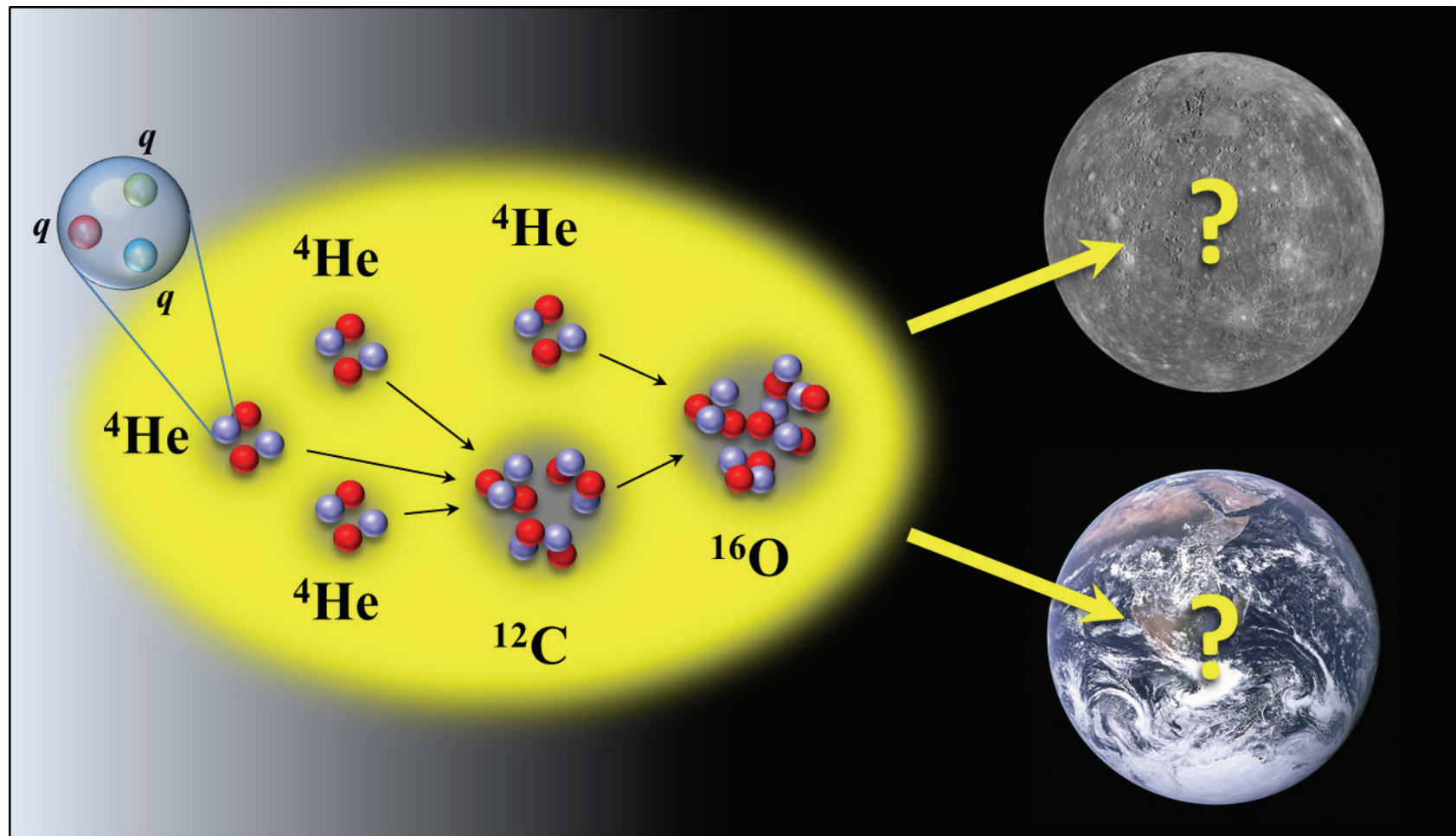
$$Z_{n_t, \text{NLO}}^{\langle O \rangle} = \langle \psi_{\text{init}} | \begin{array}{|c|c|c|} \hline \text{black} & \text{blue} & \text{yellow} & \text{blue} & \text{black} \\ \hline \end{array} | \psi_{\text{init}} \rangle$$

$$\langle O \rangle_{0, \text{NLO}} = \lim_{n_t \rightarrow \infty} Z_{n_t, \text{NLO}}^{\langle O \rangle} / Z_{n_t, \text{NLO}}$$

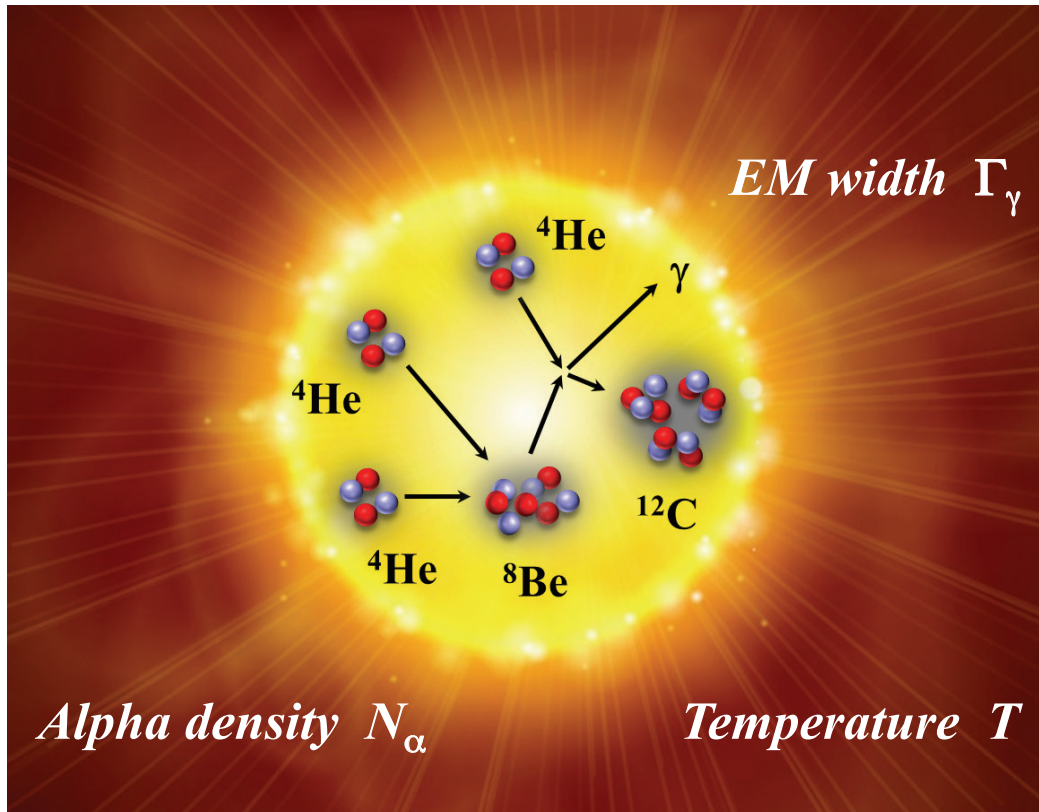
Particle clustering included automatically



Light quark mass dependence of helium burning



Triple alpha reaction rate



$$r_{3\alpha} \propto \Gamma_\gamma (N_\alpha/k_B T)^3 \times \exp(-\varepsilon/k_B T)$$

$$\varepsilon = E_h - 3E_\alpha \quad \text{Hoyle relative to triple-alpha}$$

Is nature fine-tuned?

$$\varepsilon = E_h - 3E_\alpha \approx 400 \text{ keV}$$

$$\varepsilon > 500 \text{ keV}$$

$$\varepsilon < 300 \text{ keV}$$

Less resonance enhancement.
Rate of carbon production smaller
by several orders of magnitude.
Low carbon abundance is
unfavorable for carbon-based life.

Carbon production occurs at
lower stellar temperatures and
oxygen production greatly reduced.
Low oxygen abundance is
unfavorable for carbon-based life.

Schlattl et al., Astrophys. Space Sci., 291, 27–56 (2004)

We investigate the dependence on the fundamental parameters of the standard model such as the light quark masses. Can be parameterized by the pion mass.

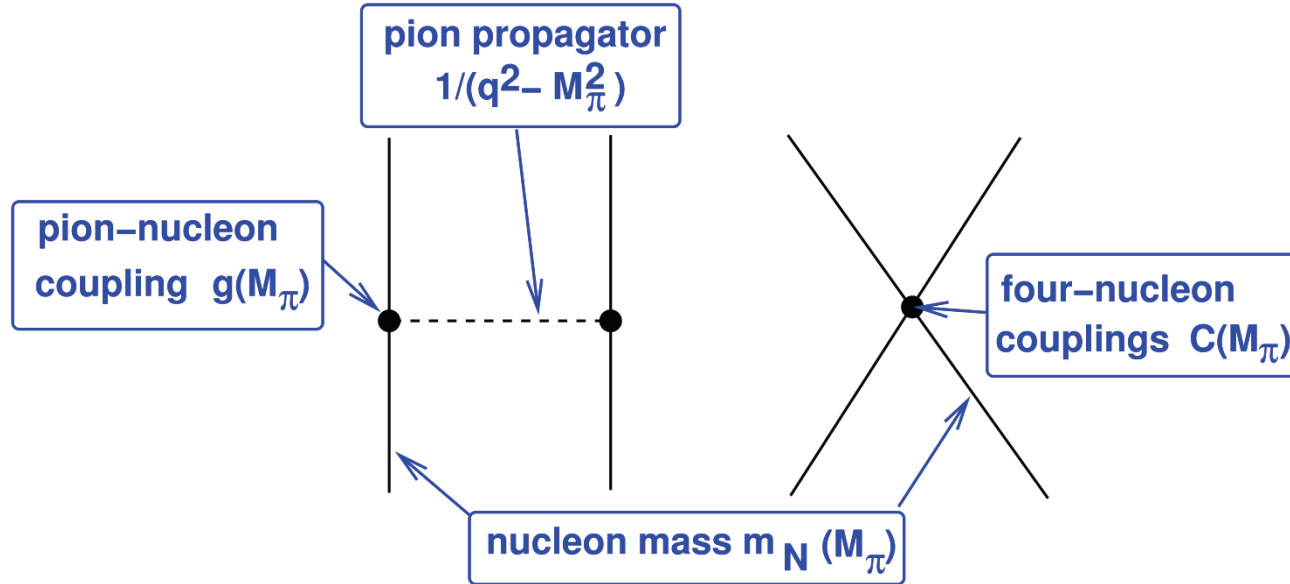
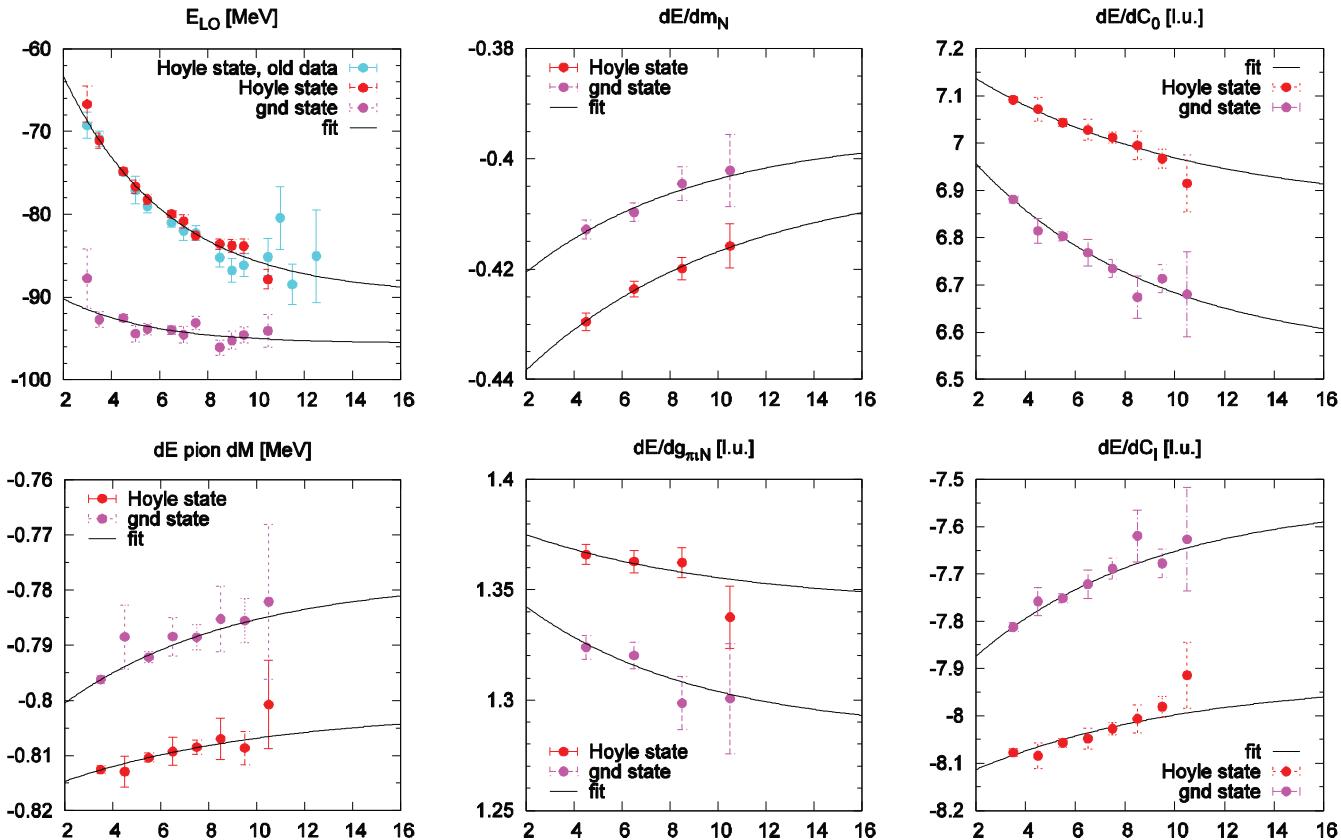


Figure courtesy of U.-G. Meißner

*Epelbaum, Krebs, Lähde, D.L, Meißner, PRL 110 (2013) 112502; ibid., EPJA 49 (2013) 82
 Berengut et al., Phys. Rev. D 87 (2013) 085018*

Lattice results for pion mass dependence



$$a = 1.97 \text{ fm}$$

$$\Delta E_h = E_h - E_b - E_\alpha \quad \text{Hoyle relative to Be-8-alpha}$$

$$\Delta E_b = E_b - 2E_\alpha \quad \text{Be-8 relative to alpha-alpha}$$

$$\varepsilon = E_h - 3E_\alpha \quad \text{Hoyle relative to triple-alpha}$$

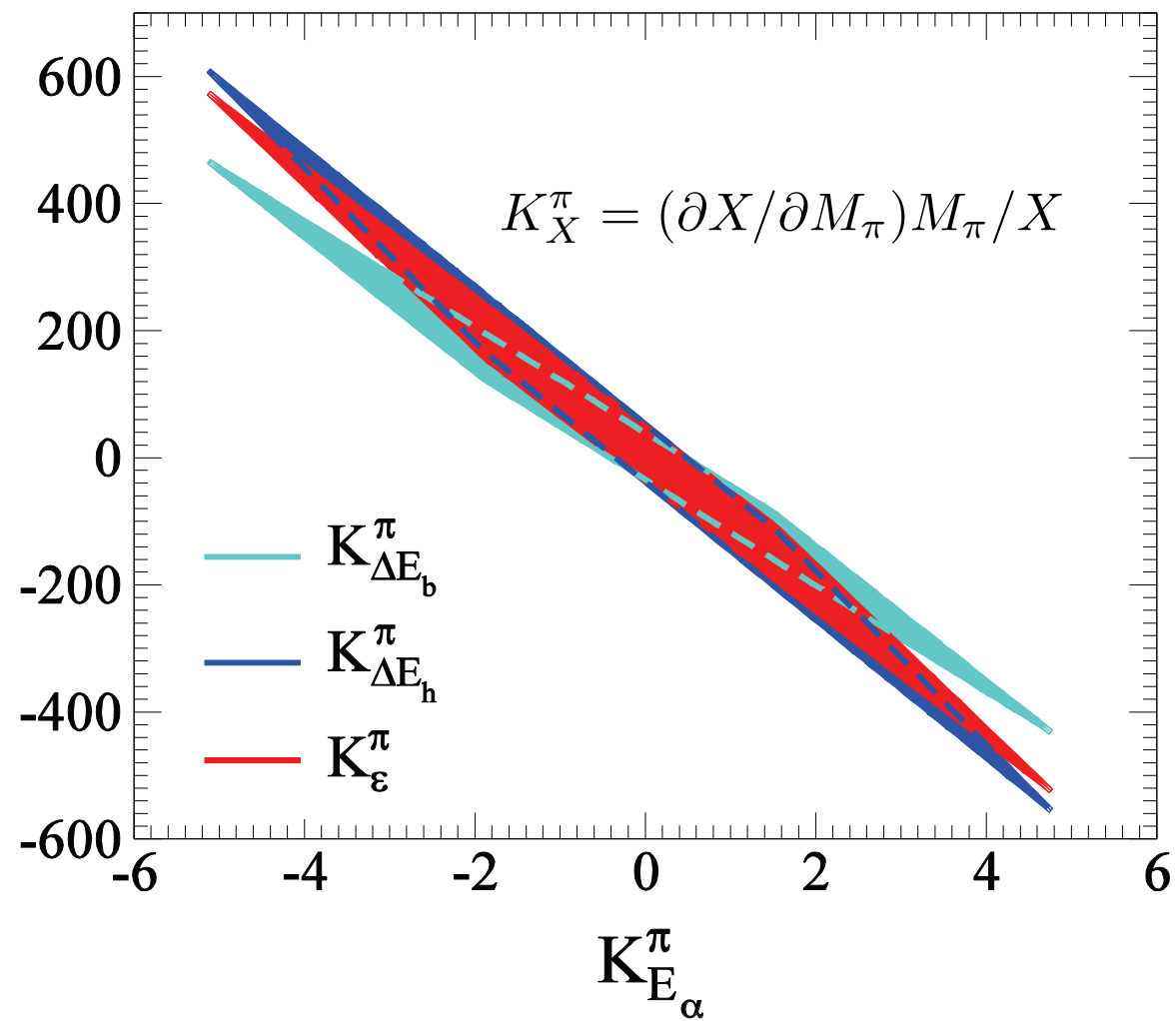
$$\frac{\partial \Delta E_h}{\partial M_\pi} \Big|_{M_\pi^{\text{ph}}} = -0.455(35) \bar{A}_s - 0.744(24) \bar{A}_t + 0.051(19)$$

$$\frac{\partial \Delta E_b}{\partial M_\pi} \Big|_{M_\pi^{\text{ph}}} = -0.117(34) \bar{A}_s - 0.189(24) \bar{A}_t + 0.013(12)$$

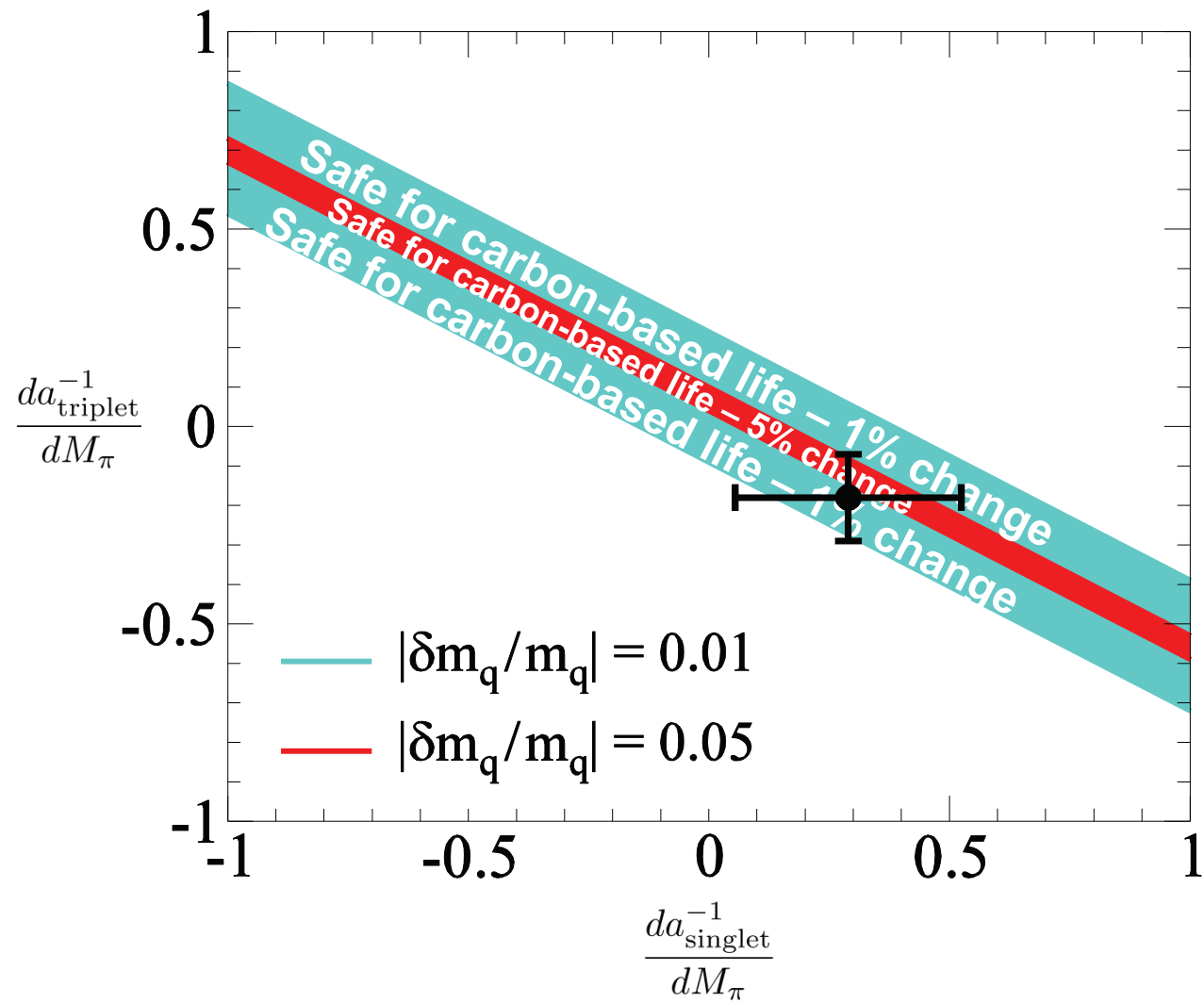
$$\frac{\partial \varepsilon}{\partial M_\pi} \Big|_{M_\pi^{\text{ph}}} = -0.572(19) \bar{A}_s - 0.933(15) \bar{A}_t + 0.064(16)$$

$$\bar{A}_s \equiv \partial a_s^{-1} / \partial M_\pi \Big|_{M_\pi^{\text{ph}}} \quad \bar{A}_t \equiv \partial a_t^{-1} / \partial M_\pi \Big|_{M_\pi^{\text{ph}}}$$

Evidence for correlation with alpha binding energy

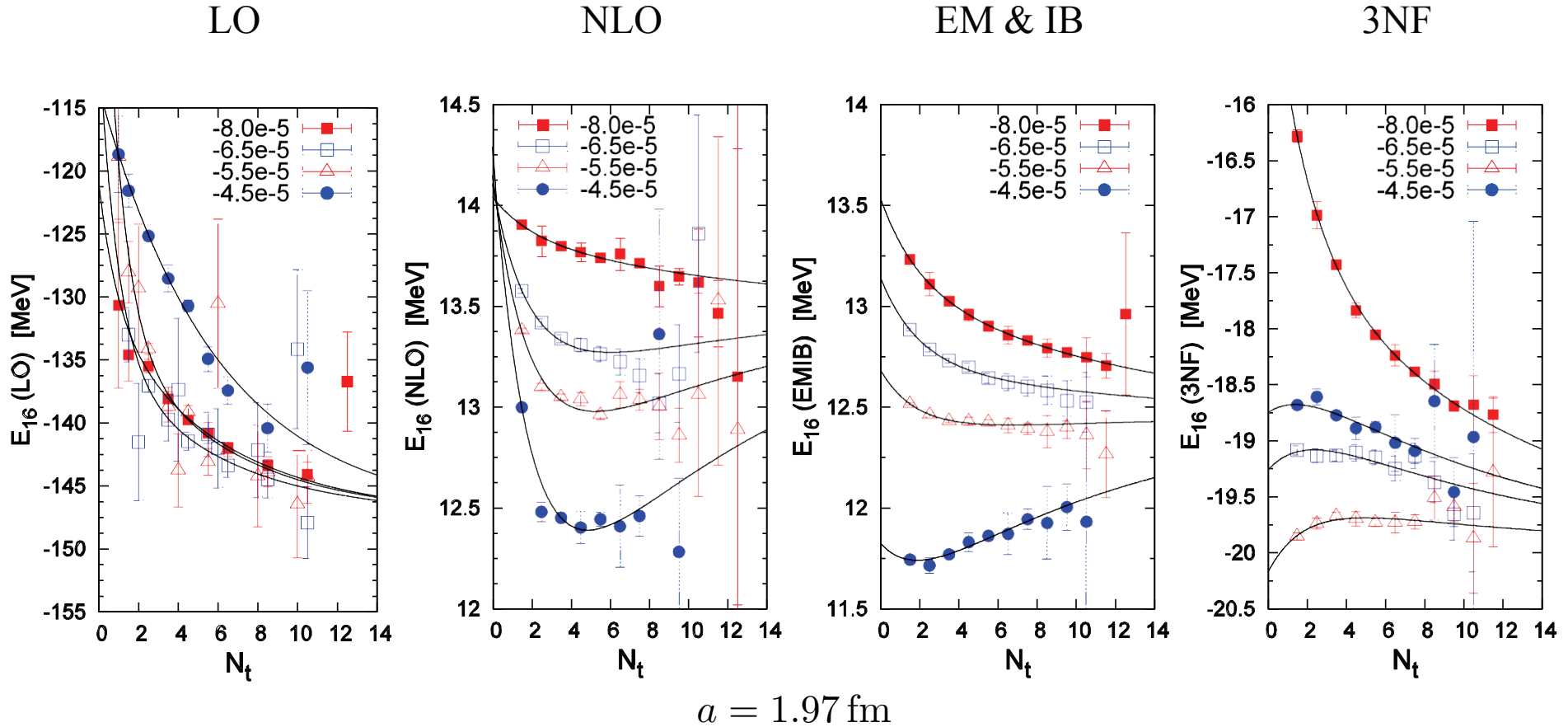


“End of the world” plot



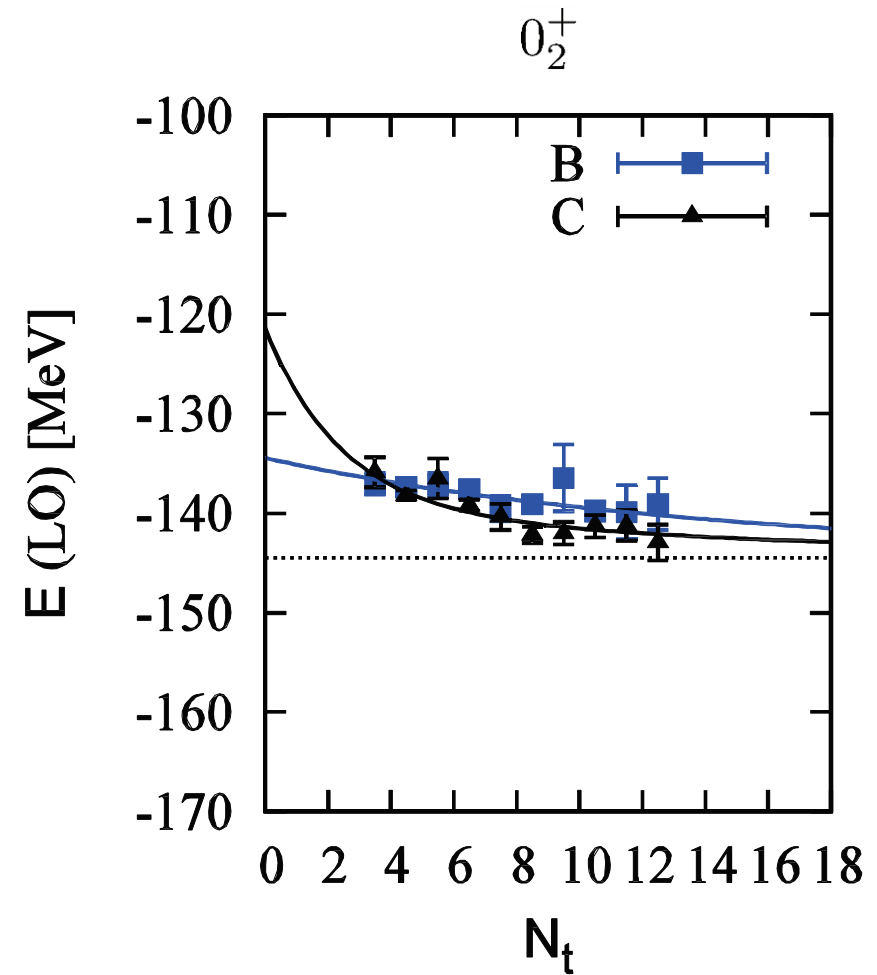
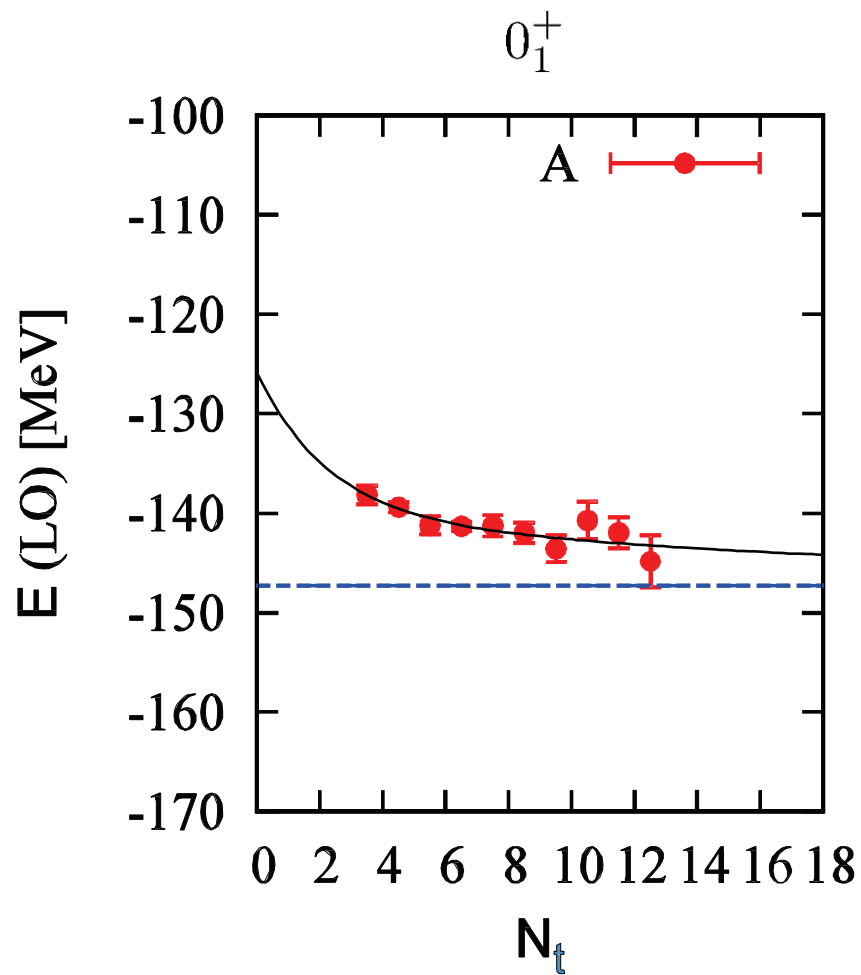
Epelbaum, Krebs, Lähde, D.L, Meißner, PRL 110 (2013) 112502; ibid., EPJA 49 (2013) 82

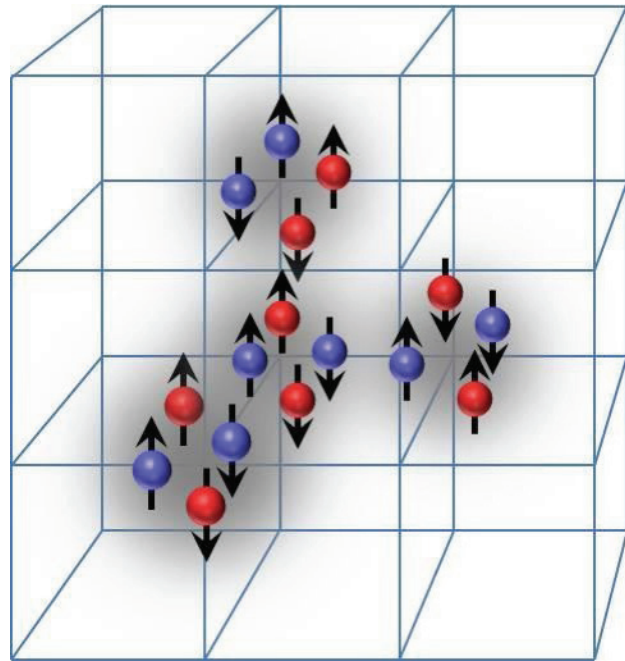
Oxygen-16 ground state



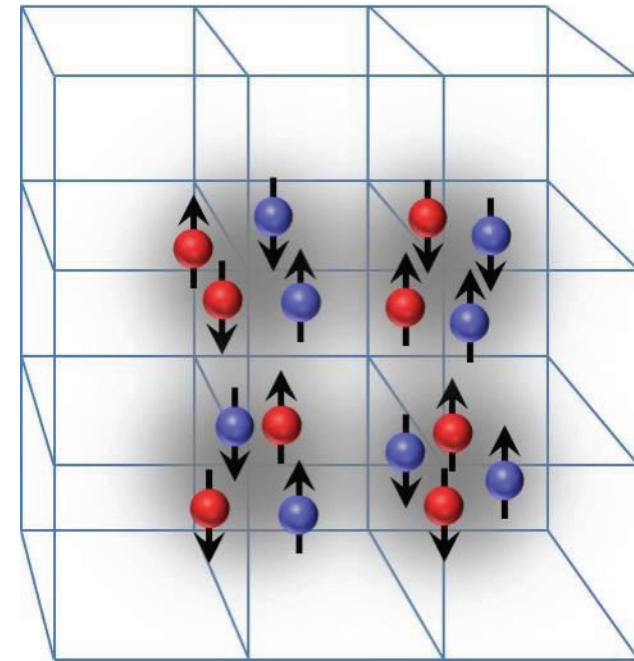
Epelbaum, Krebs, Lähde, D.L, Meißner, Rupak, PRL112, 102501 (2014)

Oxygen-16 spectrum and structure

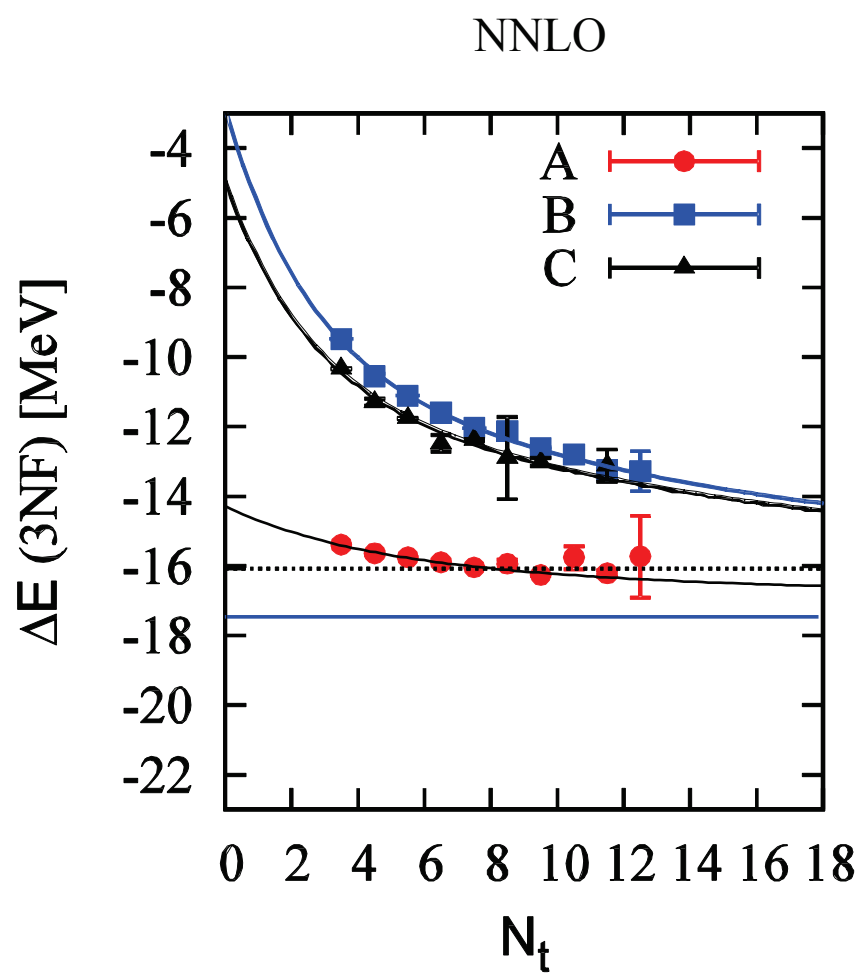
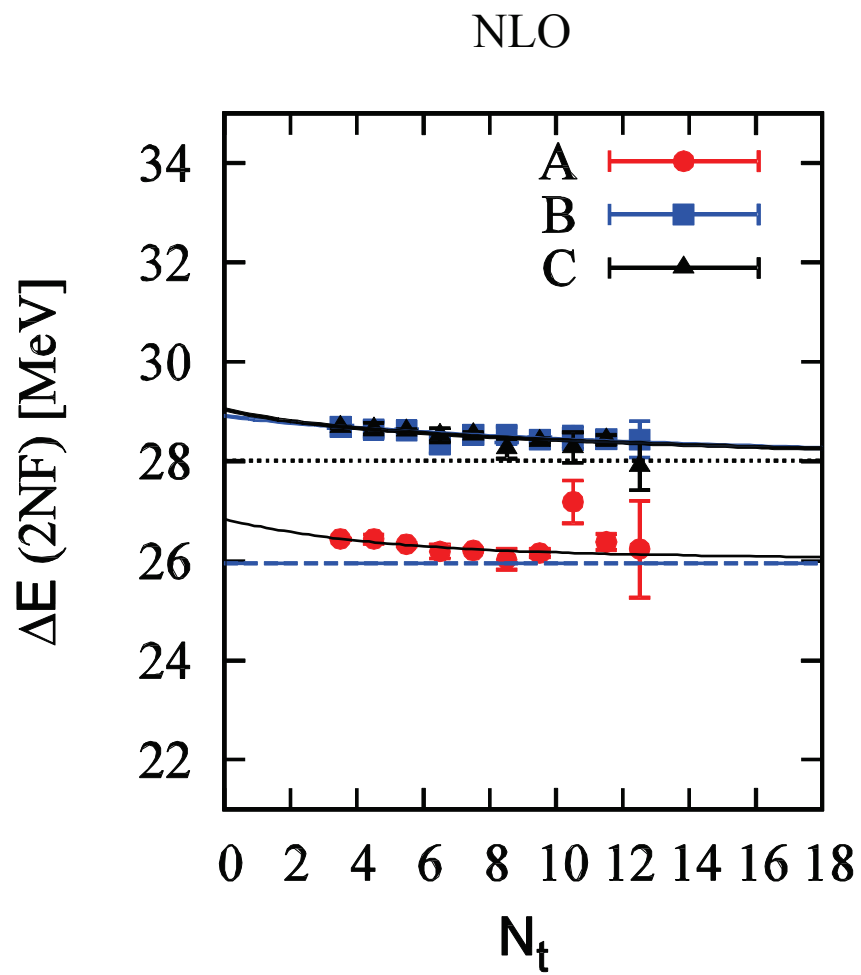


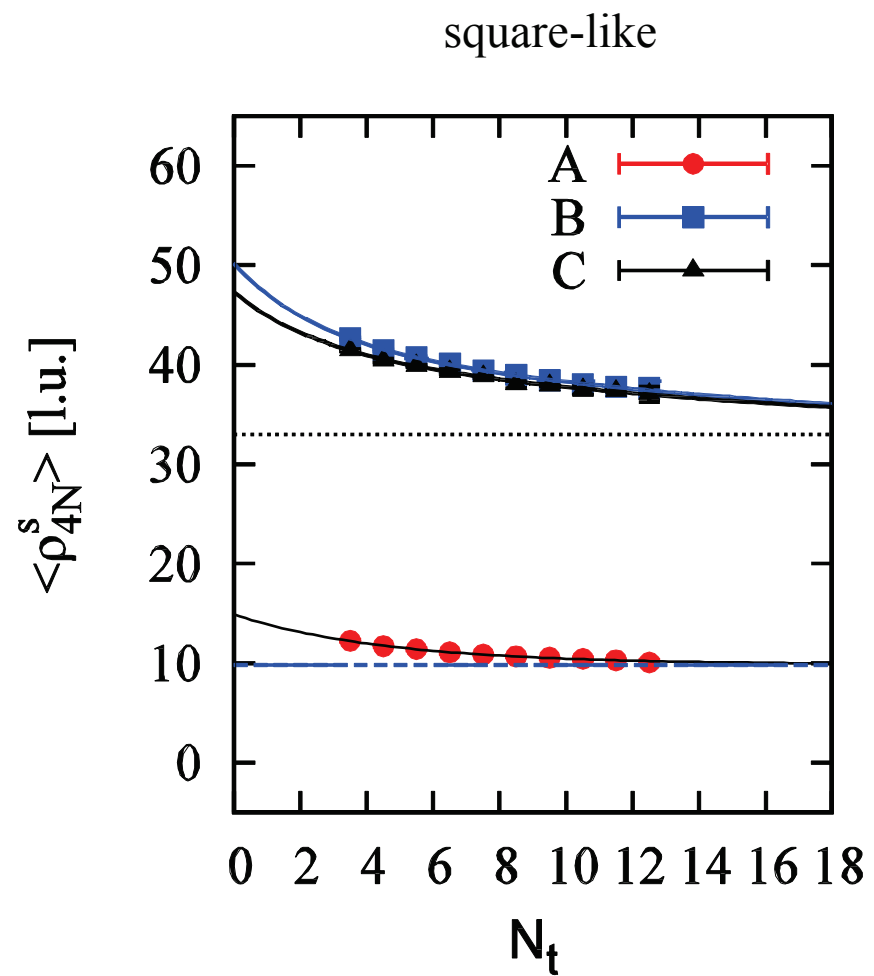
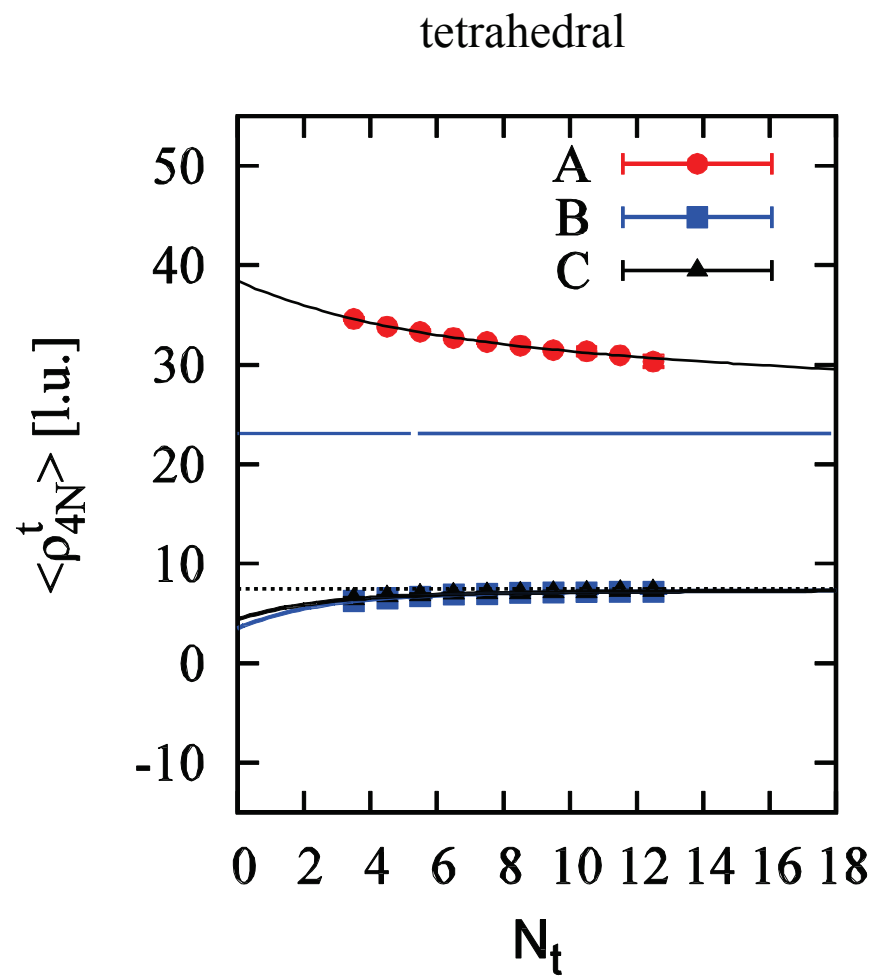
0_1^+ 

A - Tetrahedral structure

 0_2^+ 

B,C - Square-like structure





	LO	NLO	NNLO	Exp.
0_1^+	-147.3(5)	-121.4(5)	-138.8(5)	-127.62
0_2^+	-145(2)	-116(2)	-136(2)	-121.57
2_1^+	-145(2)	-116(2)	-136(2)	-120.70

We find that the overbinding is eliminated with a better NLO lattice action that fits the nuclear phase shifts to higher momenta (work in progress)

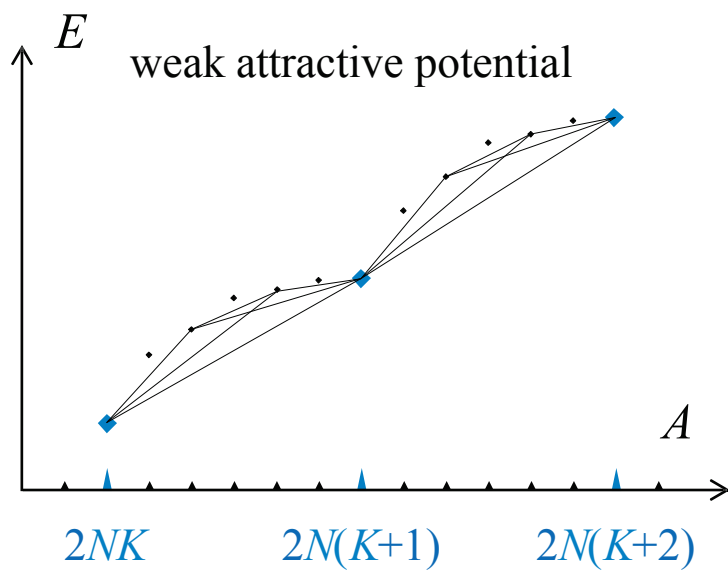
Sign oscillations

$$\begin{aligned} 1 &= (2 - 1)^{1000} \\ &= 2^{1000} - 1000 \cdot 2^{999} + \frac{1000 \cdot 999}{2} \cdot 2^{998} - \dots \end{aligned}$$

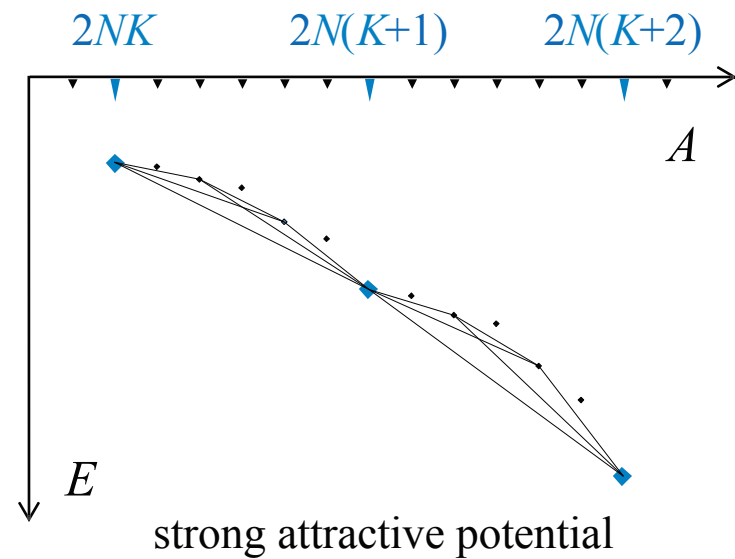
There are different types of sign oscillation problems. In explicit fermion simulations such as diffusion or Green's function Monte Carlo, the sign problem is due to Fermi statistics. In implicit fermion simulations such as auxiliary-field Monte Carlo, the sign problem is predominantly due to repulsive interactions.

Theorem: Any fermionic theory with $SU(2N)$ symmetry and two-body potential with negative semi-definite Fourier transform obeys $SU(2N)$ convexity bounds.

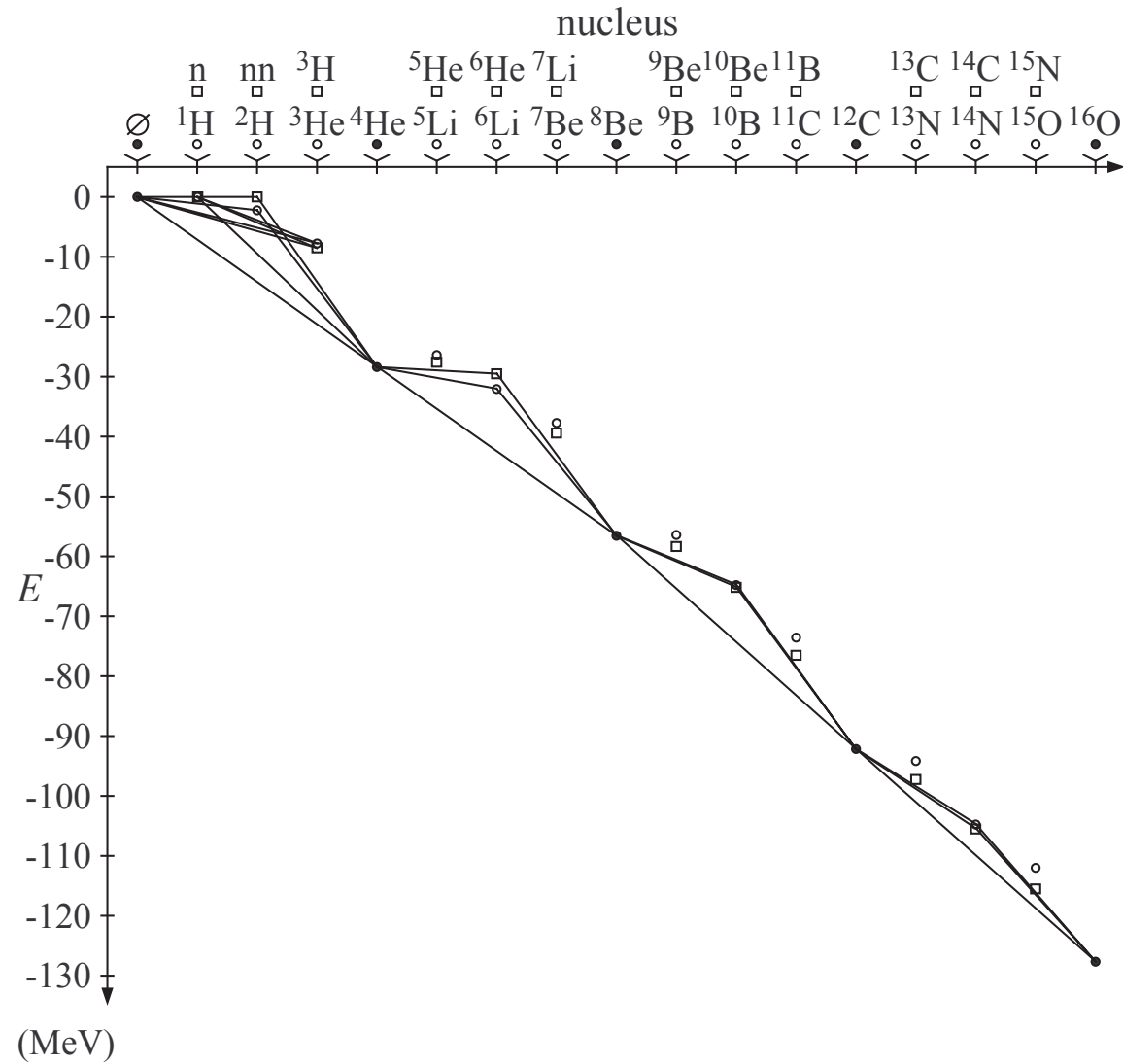
Corollary: System can be simulated without sign oscillations



Chen, D.L. Schäfer; PRL 93 (2004) 242302;
D.L., PRL 98 (2007) 182501



SU(4) convexity bounds



Symmetry Sign Extrapolation

Start with a physical Hamiltonian of interest that has a sign oscillation problem

$$H_{\text{phys}}$$

Suppose there exists some $\text{SU}(2N)$ -invariant Hamiltonian that can be tuned to reproduce the overall size, binding, and other relevant observables for the system of interest

$$H_{\text{SU}(2N)}$$

Construct a one-parameter family interpolating between the two Hamiltonians

$$H_d = (1 - d) \cdot H_{\text{SU}(2N)} + d \cdot H_{\text{phys}}$$

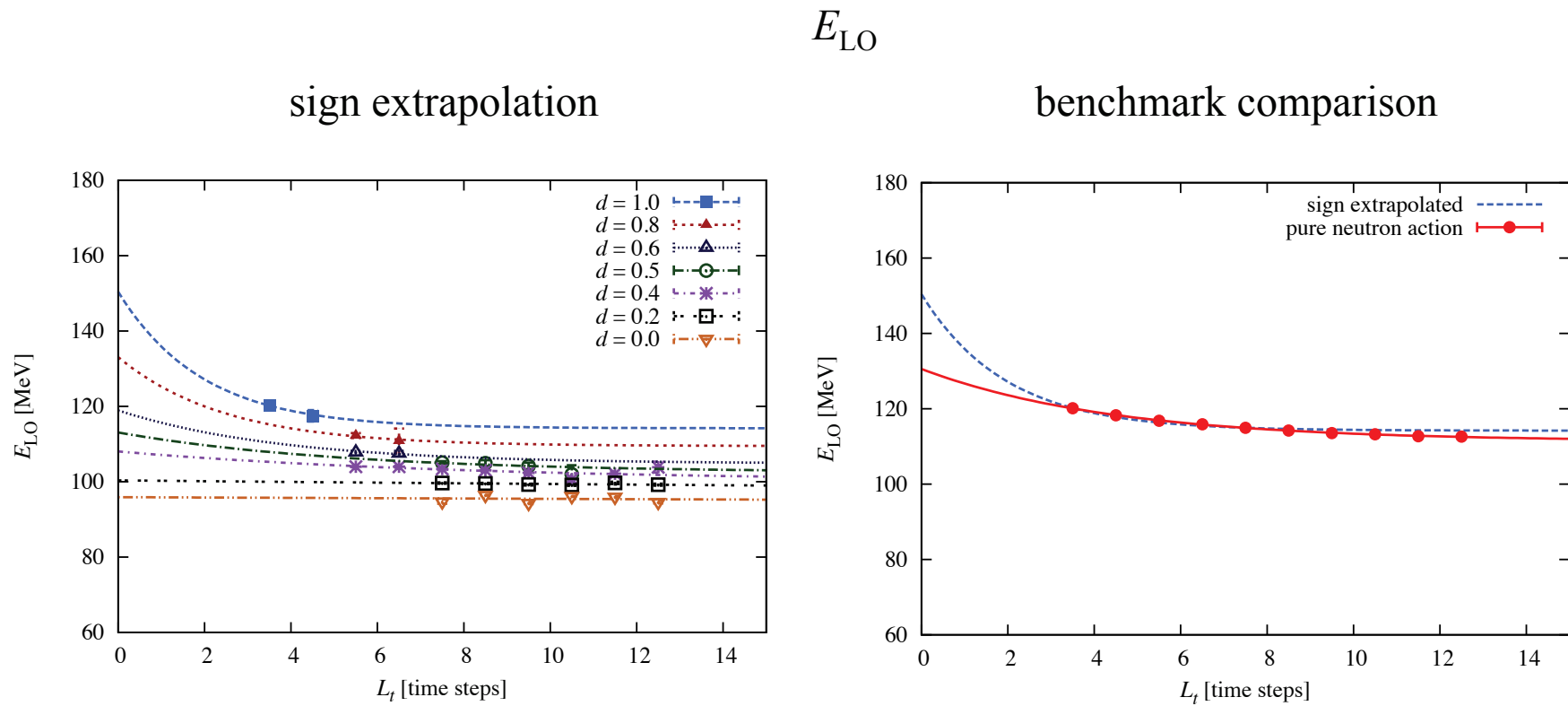
Simulations of neutron-rich matter

Pure neutron matter can be simulated using a trick which modifies the proton interactions to greatly reduce the sign problem. The modified proton interactions are allowed since there are no protons. Call this the pure neutron action.

This trick is not available for neutron-rich matter with nonzero proton fraction. But we can use pure neutron matter as a benchmark test of our sign extrapolation method.

We simulate 12 neutrons in a $(7.9 \text{ fm})^3$ periodic box using the symmetry sign extrapolation method and compare with pure neutron action results. Density is about 1/7th of nuclear matter density.

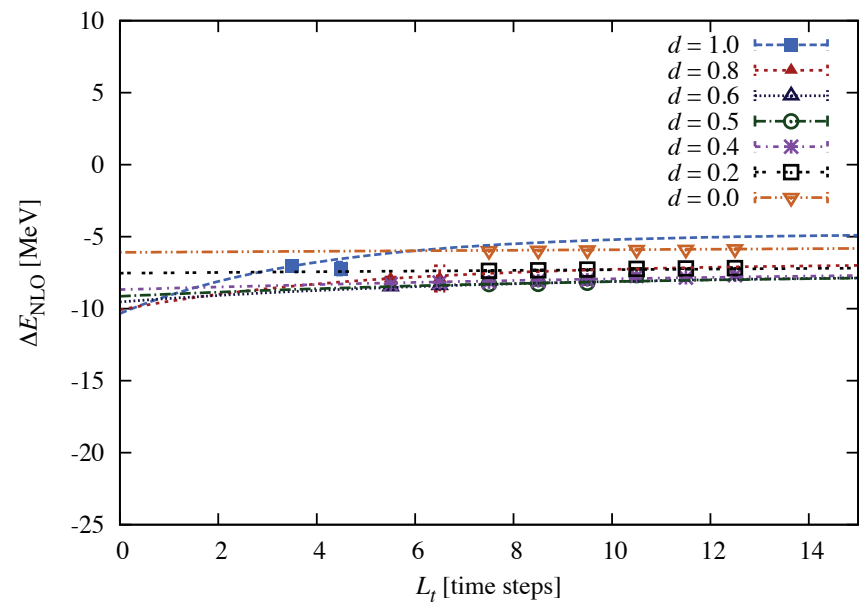
12 neutrons in $(7.9 \text{ fm})^3$ periodic box



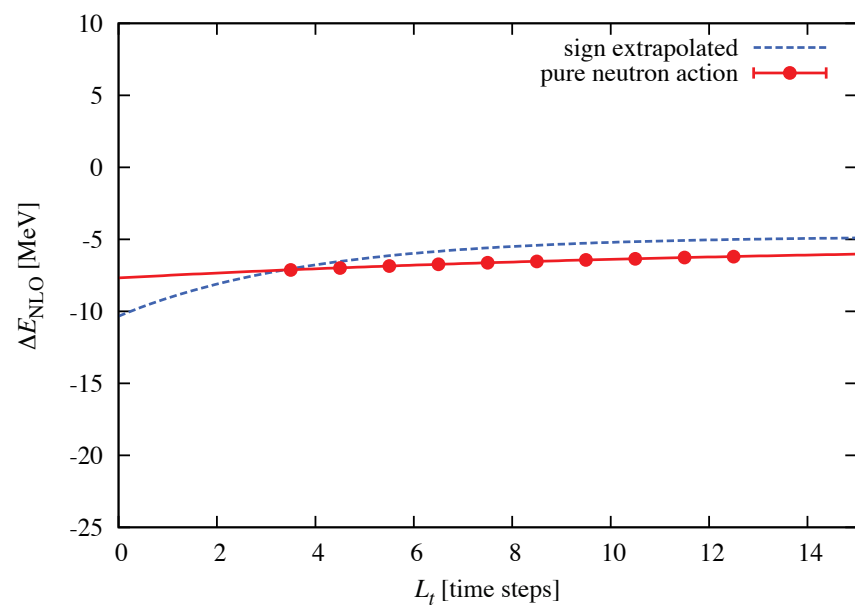
$$a = 1.97 \text{ fm}$$

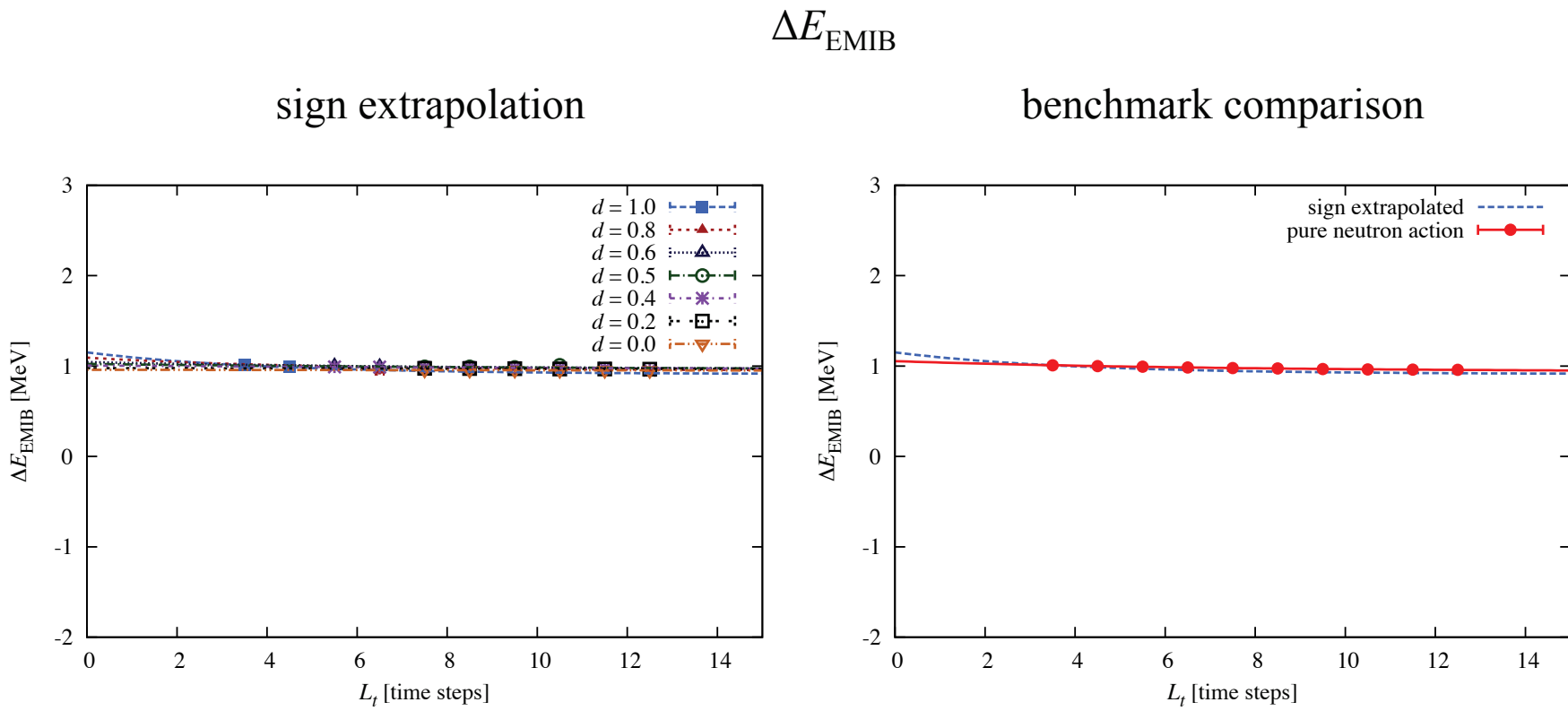
$$\Delta E_{\text{NLO}}$$

sign extrapolation



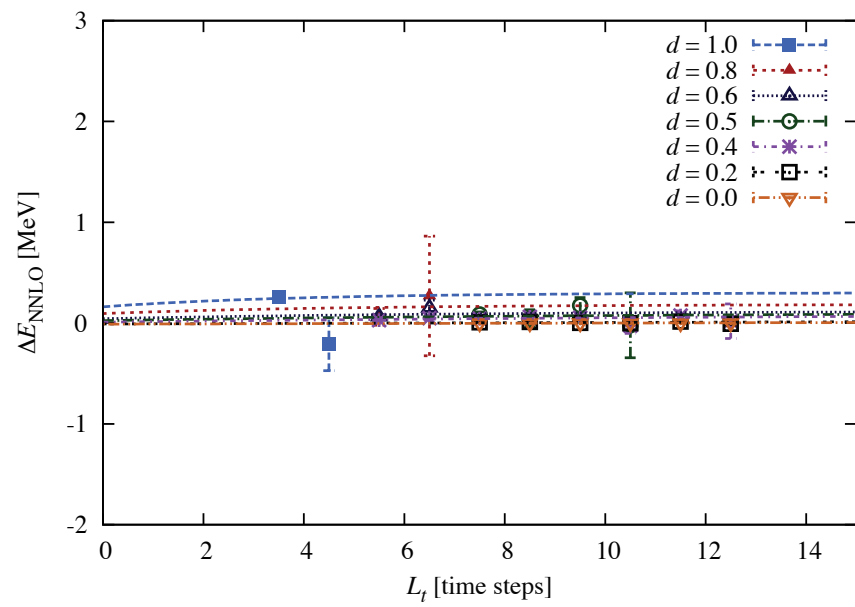
benchmark comparison



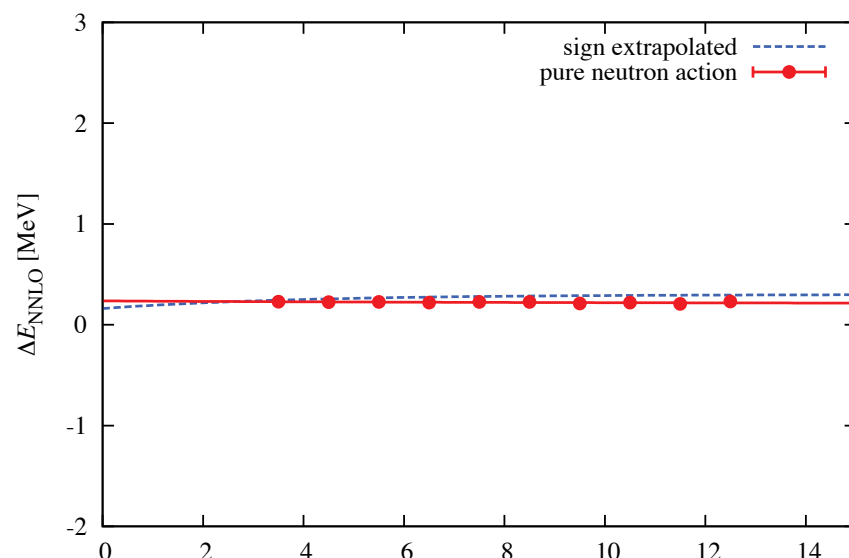


ΔE_{NNLO}

sign extrapolation



benchmark comparison



12 neutrons in $(7.9 \text{ fm})^3$ periodic box

	E_{LO} [MeV]	ΔE_{NLO} [MeV]	ΔE_{EMIB} [MeV]	ΔE_{NNLO} [MeV]
Sign extrapolation	114(6)	-4.8(5)	0.911(18)	0.30(15)
Pure neutron benchmark	111.4(2)	-5.24(8)	0.936(2)	0.21(8)

with the method tested, we now add protons...

Work in progress

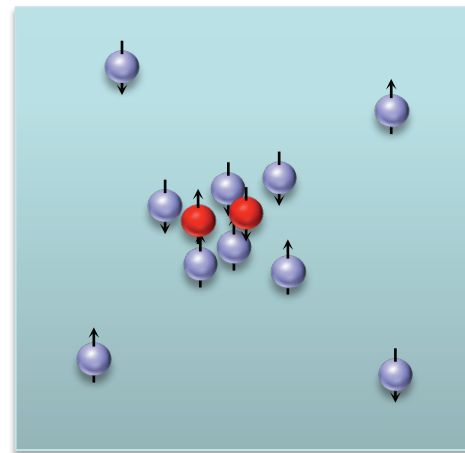
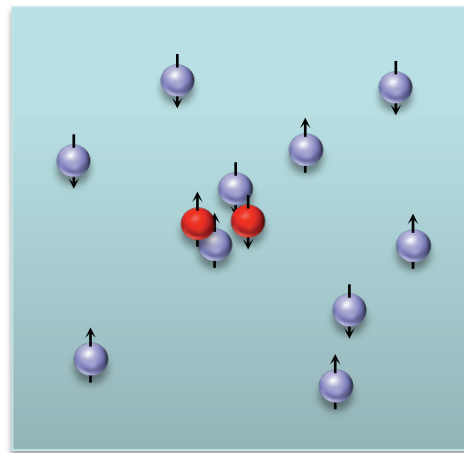
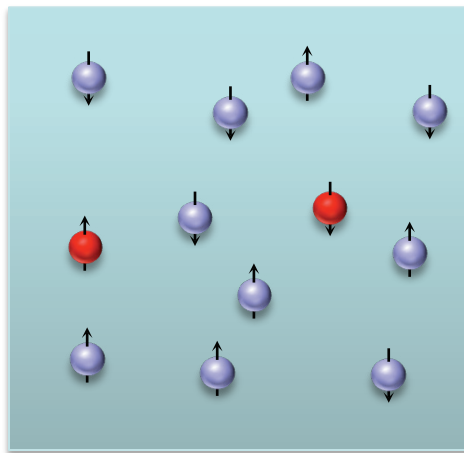
10 neutrons and 2 protons in $(7.9 \text{ fm})^3$ periodic box

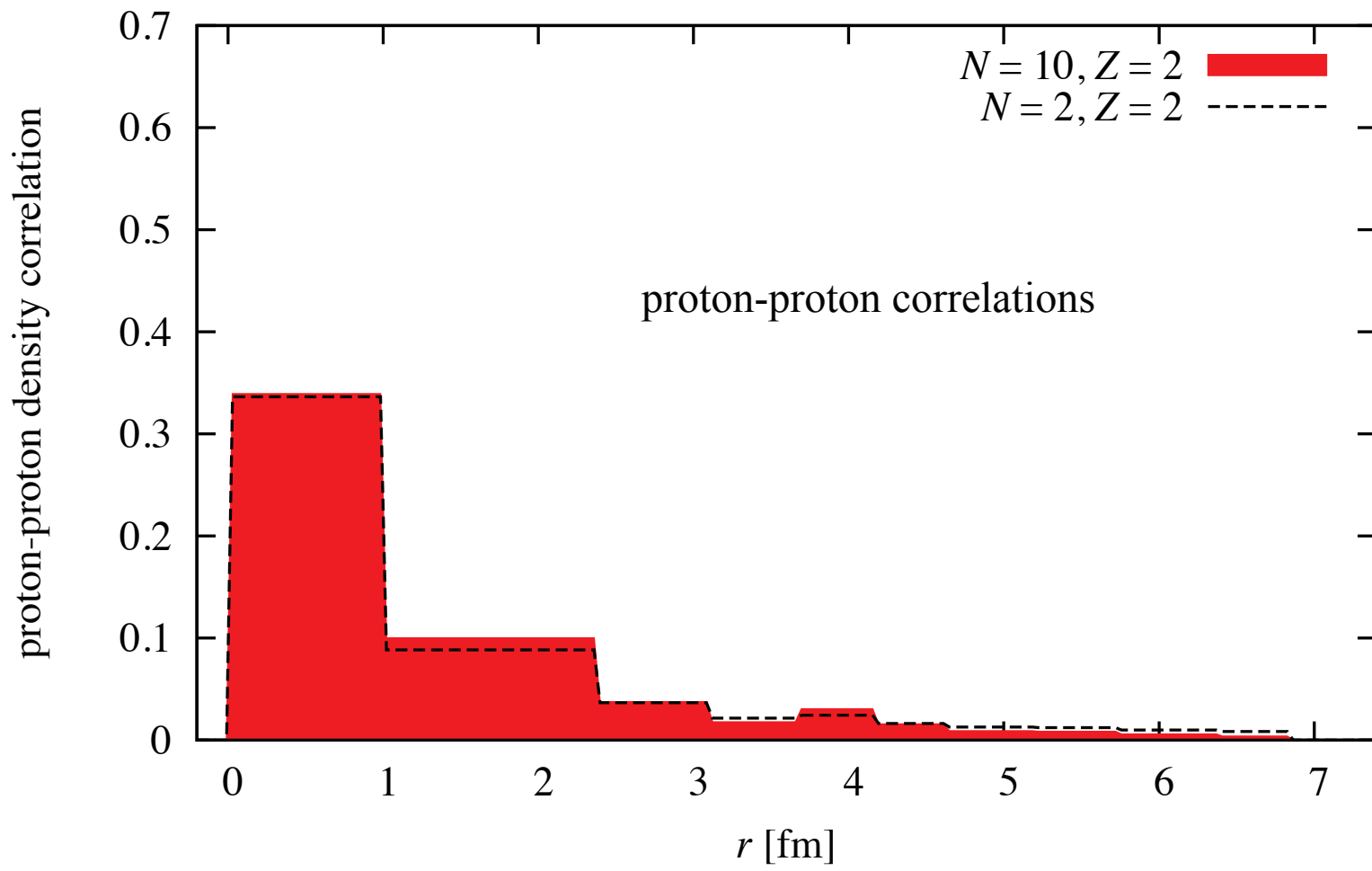
	E_{LO} [MeV]	ΔE_{NLO} [MeV]	ΔE_{EMIB} [MeV]	ΔE_{NNLO} [MeV]
Sign extrapolation	21.7(2.6)	2.15(19)	1.33(3)	-6.0(2)

$$E_{\text{NNLO}} = 19(3) \text{ MeV}$$

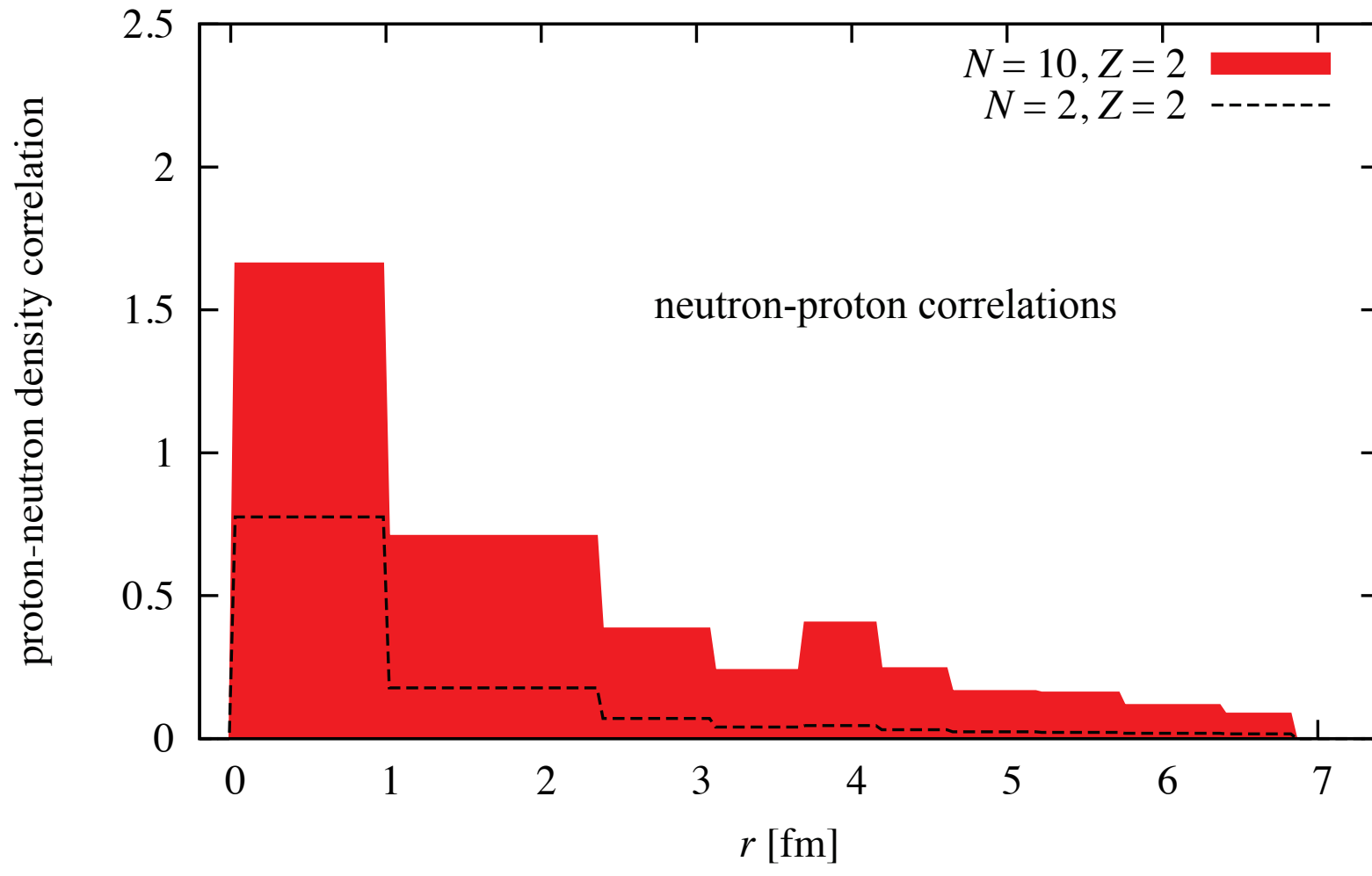
Work in progress

How are the neutrons and protons arranged?

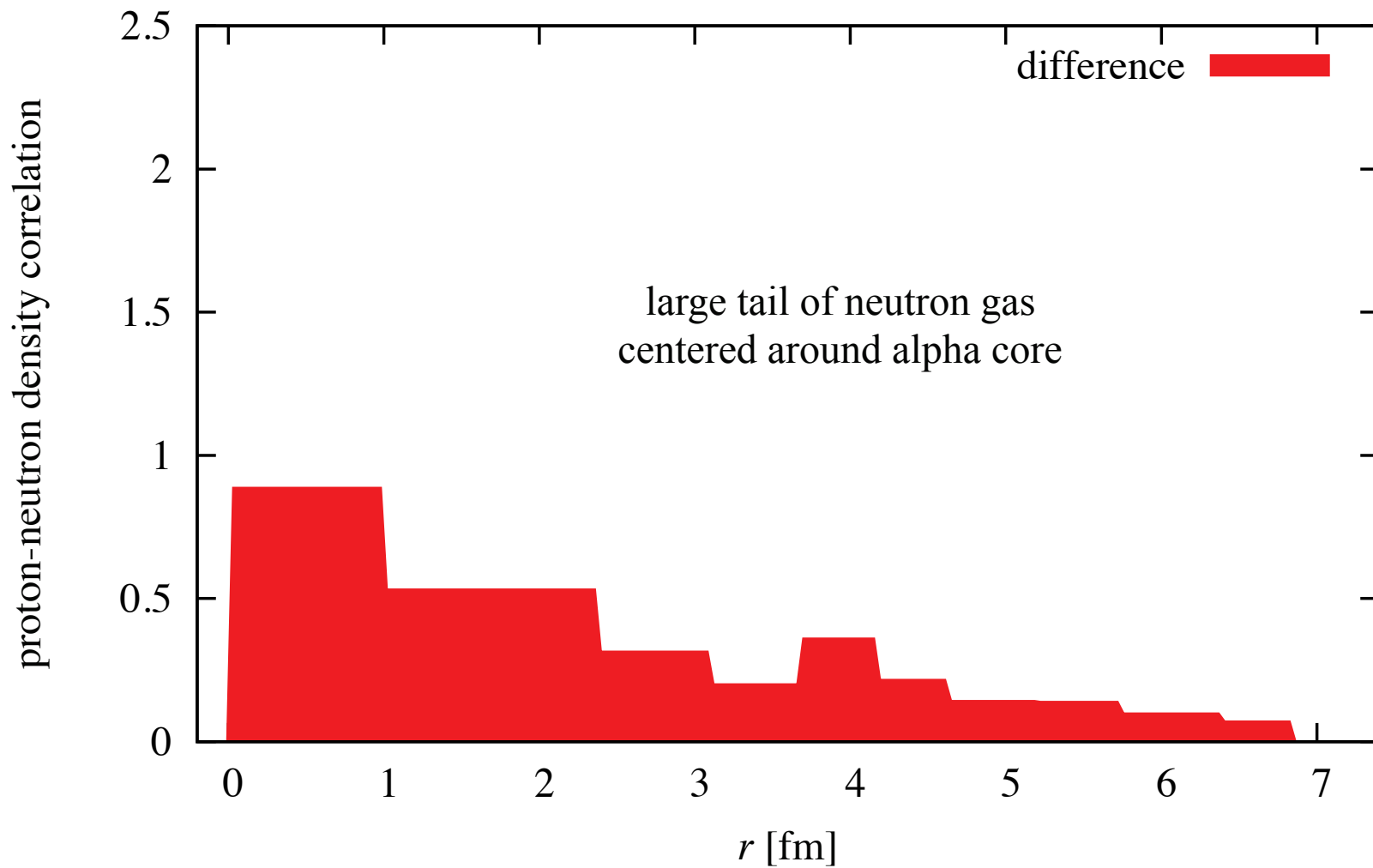




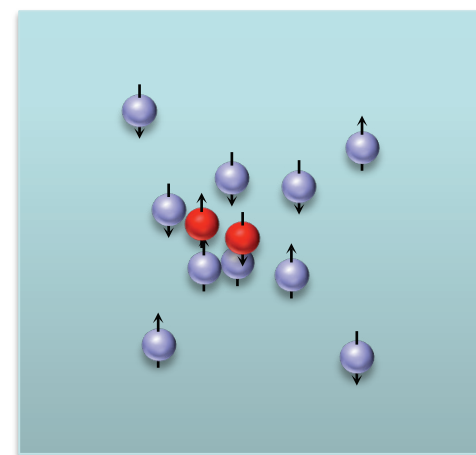
Work in progress



Work in progress

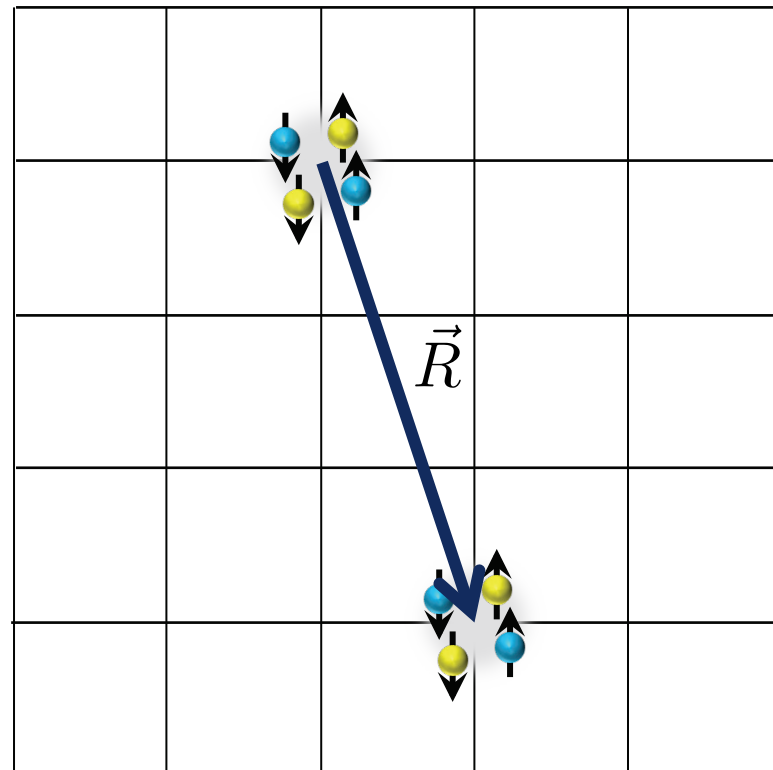


Work in progress



Adiabatic projection method

See Gautam's talk for more details



Use cluster
wavefunctions for
initial continuum
scattering states

$$|\vec{R}\rangle$$

Use projection Monte Carlo to propagate cluster wavefunctions in Euclidean time

$$|\vec{R}\rangle_t = e^{-Ht} |\vec{R}\rangle$$

$$|\vec{R}\rangle_t = \begin{array}{c} \text{[Diagram: A sequence of vertical bars representing a cluster state, with the first few bars colored blue and the rest black]} \\ | \vec{R} \rangle \end{array}$$

Construct a norm matrix and matrix of expectation values

$$\langle N \rangle_t = {}_t\langle \vec{R}' | \vec{R} \rangle_t = \langle \vec{R}' | \begin{array}{c} \text{[Diagram: A sequence of vertical bars representing a cluster state, with the first few bars colored blue and the rest black]} \\ | \vec{R} \rangle \end{array}$$

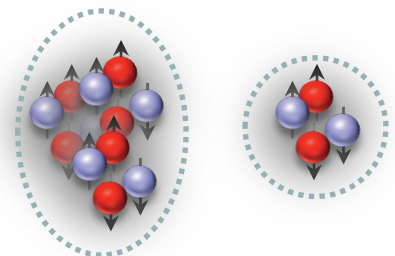
$$\langle O \rangle_t = {}_t\langle \vec{R}' | O | \vec{R} \rangle_t = \langle \vec{R}' | \begin{array}{c} \text{[Diagram: A sequence of vertical bars representing a cluster state, with the first few bars colored blue and the rest black]} \\ | \vec{R} \rangle \end{array}$$

Compute the projected adiabatic matrix

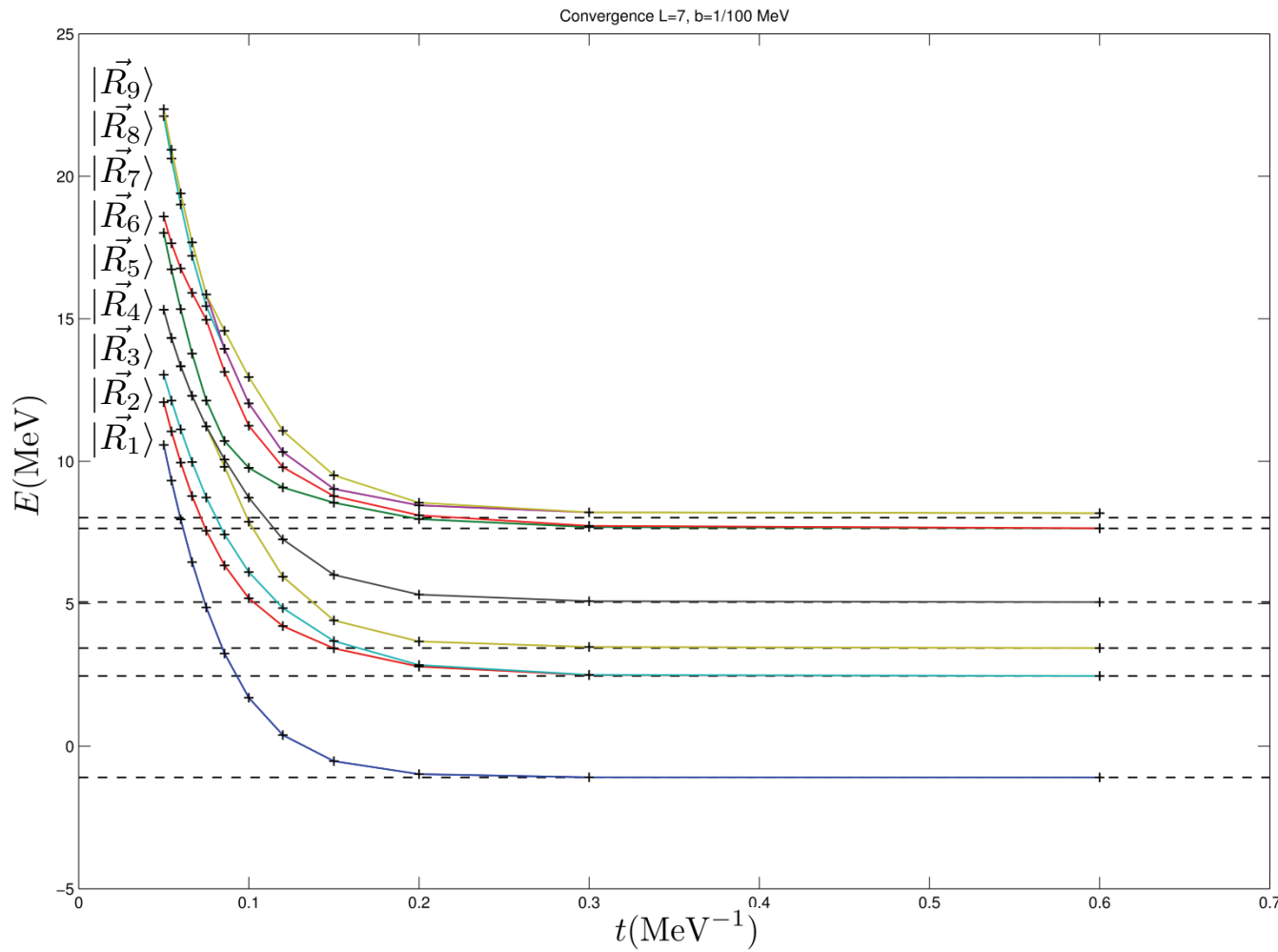
$$\langle O \rangle_{\text{adiab}} = \langle N \rangle_t^{-1/2} \langle O \rangle_t \langle N \rangle_t^{-1/2}$$

Projected adiabatic Hamiltonian is now an effective two-body Hamiltonian.
Similar in spirit to no-core shell model with resonating group method.

But some differences. Distortion of the nucleus wavefunctions is automatic due to projection in Euclidean time.

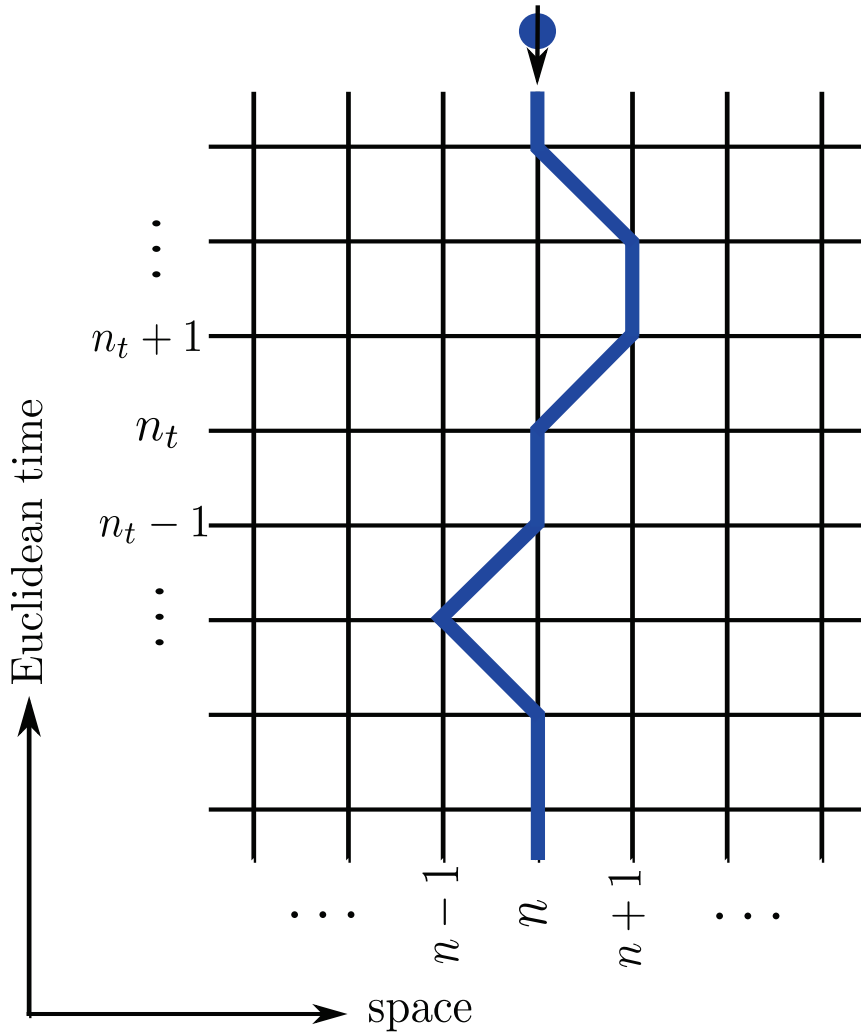


Example: Spin-quartet neutron-deuteron scattering



Pine, D.L., Rupak, EPJA 49 (2013) 151

Example: Adiabatic projection using Monte Carlo

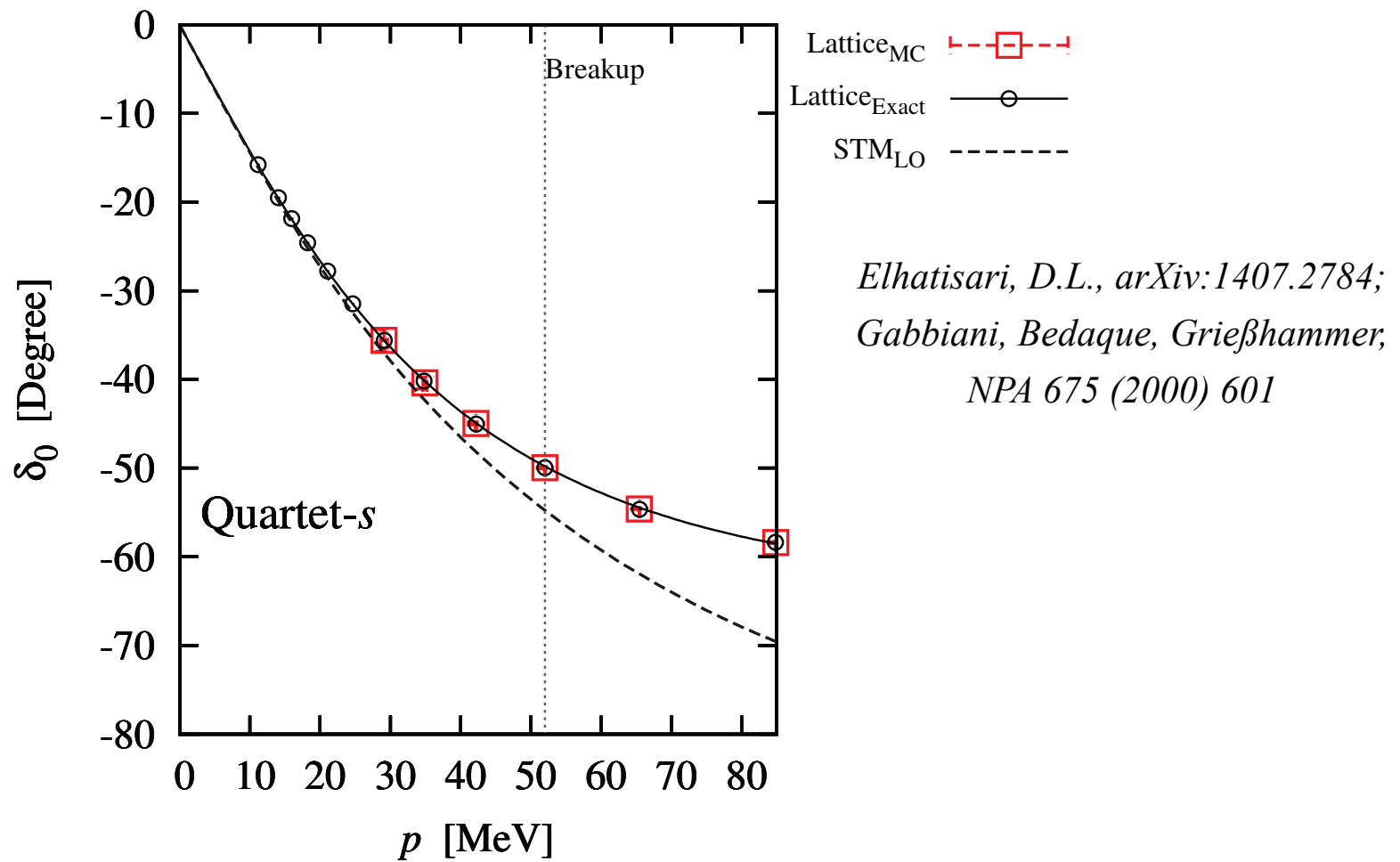


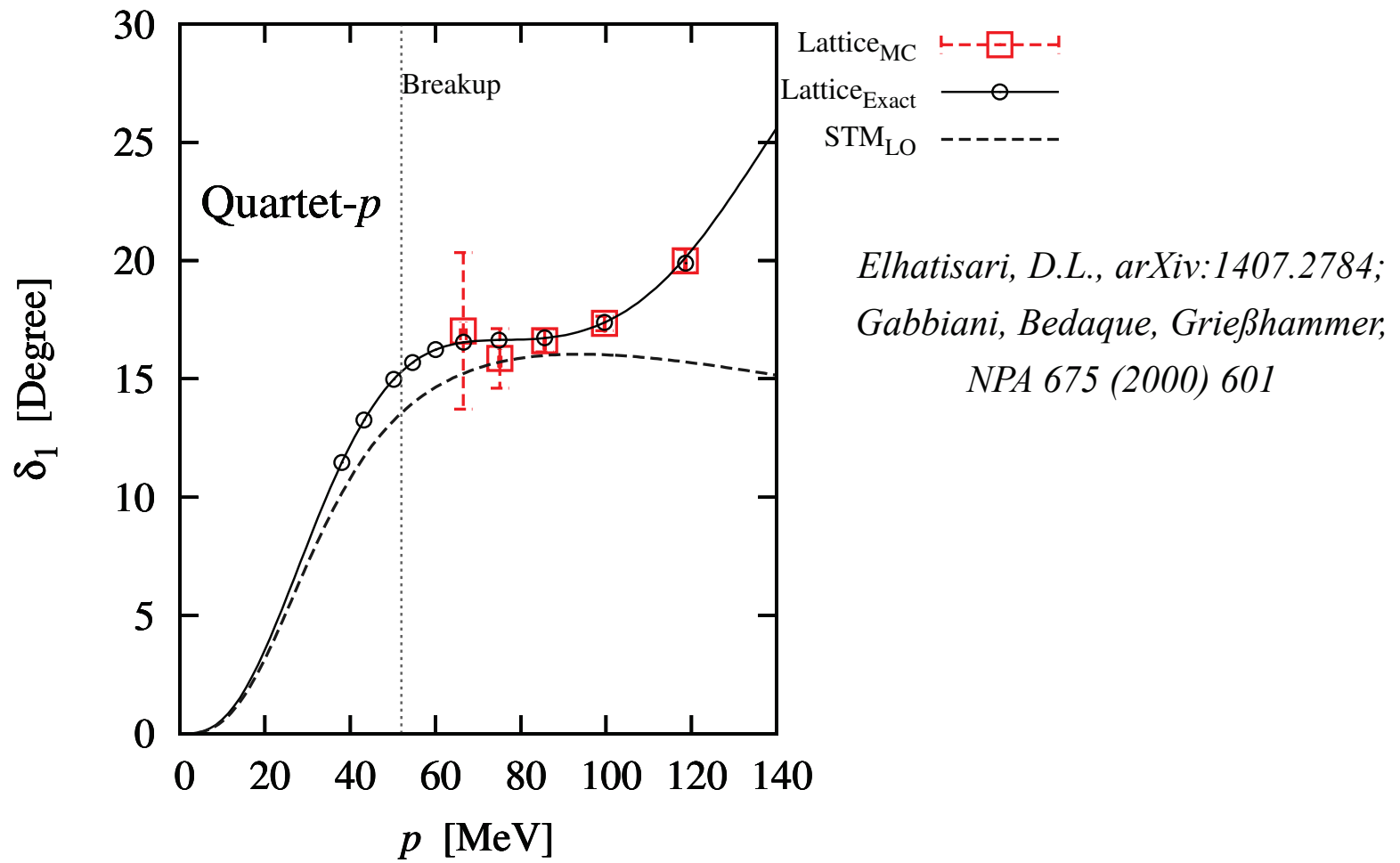
Impurity lattice Monte Carlo

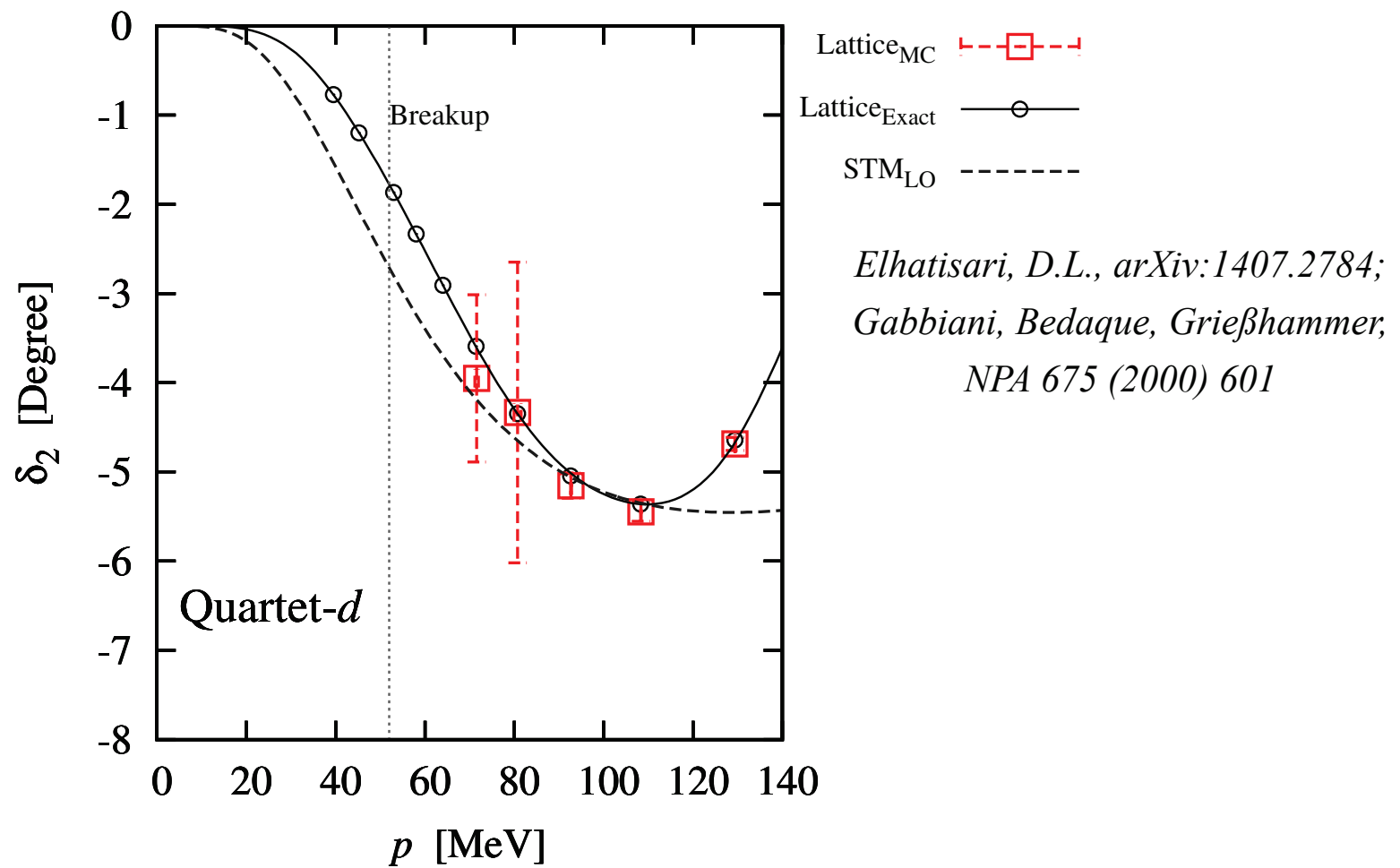
$$\langle \chi_{n_t+1}^\downarrow | \hat{M} | \chi_{n_t}^\downarrow \rangle = \left(\frac{\alpha_t}{2m} \right) : e^{-\alpha_t \hat{H}_0^\uparrow} :$$

$$\langle \chi_{n_t}^\downarrow | \hat{M} | \chi_{n_t-1}^\downarrow \rangle = \left(1 - \frac{3\alpha_t}{m} \right) : e^{-\alpha_t \hat{H}_0^\uparrow - \frac{\alpha_t C_0}{1-3\alpha_t/m} \rho_\uparrow(n)} :$$

Elhatisari, D.L., arXiv:1407.2784







Summary

A golden age for nuclear theory from first principles. Big science discoveries being made and many more around the corner.

Lattice effective field theory is a relatively new and promising tool that combines the framework of effective field theory and computational lattice methods.

Additional topics to be addressed in the near future...

Several different lattice spacings, $N \neq Z$ nuclei, adiabatic projection with hardwall boundaries for reactions, transition from S-wave to P-wave pairing in superfluid neutron matter, etc.